

**BIOLOGICAL PRINCIPLES OF CONTROL SELECTION
FOR A HUMANOID ROBOT'S DYNAMIC
BALANCE PRESERVATION**

MIOMIR VUKOBRATOVIĆ

*Mihajlo Pupin Institute, Volgina 15, 11000-Belgrade, Serbia
vuk@robot.imp.bg.ac.yu*

HUGH M. HERR

*MIT Media Lab and MIT–Harvard Division of Health Sciences and Technology,
Cambridge, Massachusetts, 02139, USA
hherr@media.mit.edu*

BRANISLAV BOROVIAC* and MIRKO RAKOVIĆ†

*Faculty of Technical Sciences, University of Novi Sad,
21000–Novi Sad, Trg D, Obradovića 6, Serbia
*borovac@uns.ns.ac.yu
†rakovicm@uns.ns.ac.yu*

MARKO POPOVIC

*MIT Media Lab, Cambridge, Massachusetts, 02139, USA
marko@media.mit.edu*

ANDREAS HOFMANN

*MIT Media Lab and Computer Science and Artificial Intelligence Lab,
Cambridge, Massachusetts, 02139, USA
hofma@csail.mit.edu*

MILOŠ JOVANOVIĆ

*Mihajlo Pupin Institute, Volgina 15, 11000–Belgrade, Serbia
milos@robot.imp.bg.ac.yu*

VELJKO POTKONJAK

*Faculty of Electrical Engineering, University of Belgrade,
11000–Belgrade, Bulevar Kralja Aleksandra 73, Serbia
potkonjak@yahoo.com*

Received 29 February 2008

Accepted 13 March 2008

This paper presents a contribution to the study of control law structures and to the selection of relevant sensory information for humanoid robots in situations where dynamic balance is jeopardized. In the example considered, the system first experiences a large disturbance, and then by an appropriate control action resumes a “normal” posture of standing on one leg. In order to examine the control laws used by humans, an experiment was performed in which a human subject was subjected to perturbations and the ensuing reactions were recorded to obtain complete information about the subject’s motion and ground reaction force. Then, a humanoid model was advanced with characteristics matching those of the experimental human subject. The whole experiment was simulated so as to achieve a simulated motion that was similar to that of the human test subject. The analysis of the control laws applied, and the behavior of selected ground reference points (ZMP, CMP and CM projection on the ground surface), provided valuable insight into balance strategies that humanoid robots might employ to better mimic the kinetics and kinematics of humans compensating for balance disturbances.

Keywords: Humanoid robot; dynamic balance; posture; large and small disturbances; balance control.

1. Introduction

Although the problem of bipedal robotic gait has been in the focus of researchers for almost 40 years, not all aspects of the gait synthesis and control have been satisfactorily addressed. Although the last several decades have seen fascinating developments in the field of legged machine locomotion, no biologically realistic movement patterns have yet been offered. In the course of any activity related to humanoid locomotion, the preservation of dynamic balance^a is of primary importance.¹

Maintenance of humanoid dynamic balance is a task that is constantly present during motion, since disturbances are present. The majority of disturbances belong to the class of small disturbances,² which are readily compensated for during the gait realization. However, disturbances of higher intensity require a special compensating action during which, for the sake of preserving dynamic balance, the gait realization can be modified or even temporarily postponed. Once the effective compensatory action prevents a fall, motion is typically resumed. Now, several questions arise: How might an appropriate compensatory action be selected in real time? What sensory information is required? On what basis should a control action be taken, bearing in mind that there might be a number of options? These are the questions to which the field has no definitive answers. Our analyses and explanations are typically focused upon one aspect of the problem, losing sight of the overall complexity of the phenomenon and the need for an all-embracing consideration of the diverse circumstances that influence the solution. In such a situation, the reaction of humans is most often of the reflex type, and is performed quickly, which gives an impression that the compensating action has not been studiously “selected”. In considering this issue one should not neglect the fact that each individual learns, practices and perfects bipedal locomotion (in all its aspects and varieties) for a long time

^aThe term “dynamically balanced” is used to refer to the condition where at least one humanoid foot, or terminal link, is flat on the ground and immobile while standing of walking.

(practically from birth), and under real conditions. During that time, a relatively large number of different control approaches have been tried, and many mistakes have been made before arriving at an effective and acceptable solution. One of the approaches by which we can try to penetrate deeper into the complexity of selecting (or forming) the compensating actions is to record how a human reacts to a certain type of disturbance, and repeat such a reaction by simulation to gain insight into the structure and parameters of the applied control laws, on the basis of which we may attempt to get a somewhat clearer picture of the criteria for selecting the type of compensatory control action to be performed.

In the literature one can find some works dealing with particular aspects of gait and the role of some fine motions. The authors of Refs. 3 and 4 observe small moments about the body's center of mass (CM) and a small spin angular momentum. In Ref. 3, the role of arms in walking is studied, and in Refs. 5 and 6, stance knee flexion. Although the maintenance of dynamic balance in the presence of disturbances is a very intriguing issue, few papers directly address the problem. In Ref. 2, according to their character, disturbances are classified as small and large, and in Ref. 7, disturbances are compensated for by controlling limb impedance, whereas in Ref. 8, the authors advocate restating the control problem using a lower-dimensional representation.

A main characteristic of a human's compensating movements is that they are most often realized by a simultaneous and very complex coordinated action of a number of joints. Such a coordinated, experience-based and precisely defined action of several joints we call a synergy. The way in which the synergetic action is performed, and how the motion might be redistributed per particular joints, are not yet known, and neither is the way in which a human decides which of the previously learnt (i.e. prepared in advance) synergies are to be applied. This problem has been tackled in Ref. 2, although it is very difficult to be sure that a control law applied to a humanoid is fully in agreement with the control law used by humans. Verification is mainly conducted according to the degree of similarity between the behaviors of a humanoid and those of a human individual in a given situation. The degree of similarity between humanoids and people is a key aspect of anthropomorphism.⁹

The way humans cope with disturbances is clearly a learnt set of behaviors, and what has been learnt is constantly subjected to testing and verification through everyday practice. Hence, how humans maintain dynamic balance, how the compensatory actions are distributed across particular joints, what indicators are used and how they are employed — all these issues are essential. In order to examine in detail the way of selecting compensatory actions as well as biomimetic control structures for overcoming disturbances, we designed a simple experiment involving a human subject standing on his left leg and leaning against a "wall" that was suddenly moved away. Because of the loss of support and the risk of a fall, the subject performed an energetic action to preserve dynamic balance. In addition to the positions (relative and absolute) of the subject's links, the intensity and position of the ground reaction force applied to his foot were measured. Then, a model was formed

of a humanoid with characteristics matching those of the experimental human subject. By analyzing the control laws that ensured that the humanoid's behaviors were close to those of the human subject, a deeper insight was obtained into the biologically inspired control schemes necessary for overcoming the disturbances acting on the humanoid. We attempted to identify the indicators on the basis of which it would be possible to choose and then to realize the appropriate compensatory control actions. The zero-moment point (ZMP) represents the indicator of dynamic balance for small disturbances, while the distance between the centroidal moment pivot (CMP) and the ZMP represents the existence of a nonzero horizontal moment acting about the humanoid's CM. In this investigation we consider the roles of the ZMP and CMP ground reference points when a large disturbance is applied to a human while he is standing.

2. Indicators of Foot Dynamic Balance and of Motion Anthropomorphism — Basic Ground Reference Points

2.1. ZMP

When walking, a humanoid robot must maintain control over its CM (position, velocity and acceleration) in the presence of gravity, and possible force disturbances. It must move its CM to avoid obstacles, move its feet to take steps, and move its hands to manipulate objects. Hence the motion required is determined, to a large extent, by the environment in which the robot operates. We call the coordinated movement of the robot in terms of its workspace coordinates (movement of its CM, hands, feet) the *external synergy*.¹ Further, we call the coordinated movement of the robot in terms of its joint coordinates the *internal synergy*.¹ In order to determine the internal synergy that will produce the desired external synergy, it is necessary to establish a relationship between these two coordinate spaces. A special aspect of this problem for bipedal walking robots, which does not occur in the case of fixed-base manipulators, is the fact that all joints of the bipedal robot are powered and directly controllable except for the “joint” that represents contact with the ground. This lack of control at the ground contact interface makes a walking robot *underactuated*. Hence, a bipedal robot may fall due to an external disturbance, or due to an incorrect action of the robot itself.

One critical strategy for preventing a humanoid from falling is to take control actions at the actuated joints that ensure a desired contact of the foot with the ground. In the lateral direction, this often means ensuring that the foot does not roll on an edge (to avoid twisting the ankle). In the forward direction, while the humanoid is standing, this means that the foot should be flat on the ground. In the forward direction, while the humanoid is walking in the single support phase, this means that the foot is flat on the ground during the first portion of the stance phase, and that the ball of the foot is flat on the ground (but the heel is off the ground) during the subsequent portion of the stance phase. Such ground contact requirements act to constrain the relationship between the internal and external synergies.

The ZMP was introduced by Vukobratović together with his closest associates.^{10–15} The first application of the ZMP was made by Japanese scientists in the middle of the 1970s, guided by the father of robotics in Japan, the late professor Kato. If we consider regular walking,¹ in practice the ZMP indicates whether a robot foot, or the foot’s terminal link, is immobile and in full contact with the ground surface during the single support phase. The ZMP can be defined in several ways. Consider a Cartesian frame with the x - and y -axes being tangential to the flat ground and the z -axis being normal. During the single support phase of walking there is always a unique point for which $\Sigma M_x = 0$ and $\Sigma M_y = 0$, where M is the moment about an axis generated by the ground reaction forces — because these forces can only push and not pull the foot or terminal link. The point inside the support area (excluding its edges) for which this relation holds is called the ZMP. Therefore the ZMP, if it exists, represents the point of resulting reaction forces at the contact surface between the extremity and the ground, indicating that the foot or terminal link is not rotating about its edge. Alternatively, instead of a summation of ground reaction forces, one may sum the forces applied by the robot against the ground surface. The ZMP can then be thought of as that point inside the support area at which the net moment due to gravitation and all inertial forces induced by the mechanism’s motion (and additional external forces if they exist) has no component along the horizontal axes. The ZMP as a function of the CM position, net CM force ($F = M \cdot a_{CM}$), and net moment about the CM can be expressed as

$$\begin{aligned} x_{ZMP} &= x_{CM} - \frac{F_x}{F_z + Mg} z_{CM} - \frac{M_y(r_{CM})}{F_z + Mg}, \\ y_{ZMP} &= y_{CM} - \frac{F_y}{F_z + Mg} z_{CM} + \frac{M_x(r_{CM})}{F_z + Mg}, \end{aligned} \tag{1}$$

where M is body mass, $M_x(r_{CM})$ and $M_y(r_{CM})$ are components of the moment about the CM and g is the gravitational constant. Equation (1) defines the ZMP location on the ground within the support area in either the single or the double support phase.^b During the single support phase, a ZMP location within the support area indicates that the robot’s stance foot is immobile and in full contact with the ground. However, in the double support phase, the ZMP cannot identify whether one foot has rotated about its edge. Since such an event is rather important to detect, one should separately consider each foot and its contact with the ground. Accordingly, one must consider two center-of-pressure points, CoP_{left} and CoP_{right} , where vertical ground reactions F_{GRleft} and $F_{GRright}$ act on the left and the right foot, respectively. The CoP, measured independently on each humanoid

^bBy definition, in the double support phase there are two feet in contact with the ground, and accordingly there are two ground reaction forces acting, one force for each foot. However, those two forces can be summed and replaced by a single resultant force. The point at which this resultant force pierces the ground surface is the ZMP. It should be noted that in the double support and single support phases, there exists only one ZMP.

foot, indicates whether at least one robot foot, or the foot's terminal link, is immobile and in full contact with the ground surface in double support. In summary, during the single support phase, the ZMP can be used to indicate whether the robot's stance foot, or terminal link, is immobile and in full contact with the ground, but in the double support phase one may consider three ground reference points, namely CoP_{left} , $\text{CoP}_{\text{right}}$, and the ZMP. The third point, ZMP, can be derived from the two CoP points (left and right) and the corresponding intensities of ground reactions (F_{GRleft} and F_{GRright}).^c

Consider first a humanoid in a single support standing posture having a one-link foot. The sole of the supporting leg is in static contact with the ground over its entire area. In this case, the ZMP is inside the support area, and the foot remains flat on the ground. We use the term "dynamically balanced" to refer to this condition when the foot, or terminal link, is flat on the ground and immobile. Dynamic balance is achieved when the foot is not slipping and the ZMP is inside the support area (excluding its edges). Having in mind that during the single support phase of walking, the real-time ZMP position can be easily acquired by pressure or force sensors located at or near the sole, it is clear that, as an indicator of dynamic balance of a humanoid in the presence of disturbances, use of ZMP feedback is indispensable and sufficient.^d

Significant disturbances can result in situations where the humanoid cannot maintain a desired foot-ground interaction. Suppose that a disturbance has occurred, and the foot begins undesirably to roll (one side of the sole begins separating from the ground). This is typically an undesirable condition, particularly if the roll is in the lateral direction. That is to say, the uncontrolled rolling may contribute in an undesirable way to the humanoid's external synergy. If foot roll occurs, the ZMP moves to the edge of the foot. In this situation, the ZMP no longer exists and the humanoid is in a state of "dynamic imbalance".

Note that these considerations are valid for a two-link foot, as well as a one-link foot. A two-link foot, with a joint at the ball of the foot before the toes, is often useful for more accurately modeling human walking. During the heel-off phase of the walking cycle, the heel comes off the ground, and the back link of the foot has "rolled" about the joint at the ball of the foot. However, the front link (representing the toes and area forward of the joint at the ball of the foot), in the case of a dynamically balanced system, remains immobile and flat on the ground until the moment of toe-off, when the foot begins stepping. If disturbances are applied to such a system, the ZMP can be used to indicate whether a system remains dynamically balanced or, in this case, whether the forefoot remains immobile and flat on the ground surface.

^cThe ZMP is an overall indicator of dynamic balance while the CoP points provide critical information as to whether a particular foot is immobile and in full contact with the walking surface.

^dThis assumes, of course, that the stance foot does not slide on the ground surface, such as might occur if a humanoid steps onto a patch of ice.

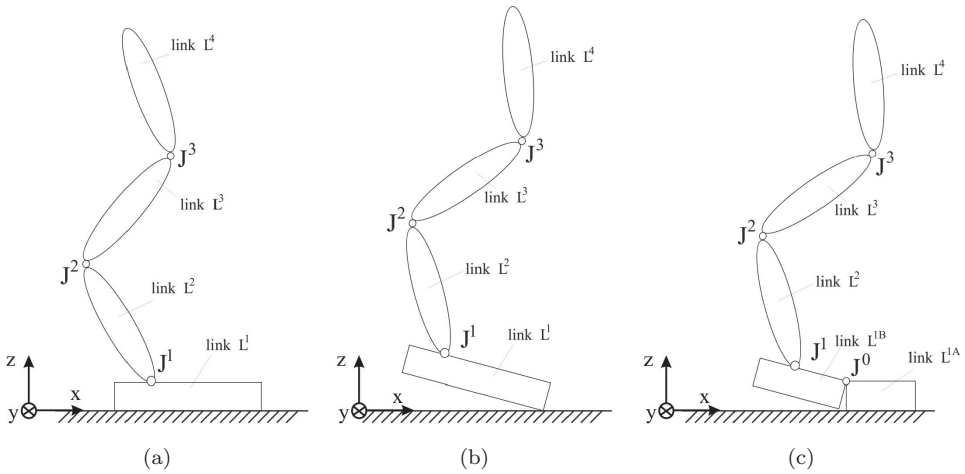


Fig. 1. Illustration of the notion of foot or terminal link dynamic balance.

Consider the four-link physical inverted pendulum, supported on the ground by its bottom link (Fig. 1). The joints of the pendulum, J^1, J^2 and J^3 , are powered. If links L^2, L^3 and L^4 move such that link L^1 remains immobile with respect to the ground (Fig. 1(a)), then we say that the foot or terminal link is dynamically balanced. However, if the motion of L^2, L^3 and L^4 causes L^1 to move and to lose contact with the ground (heel contact, as shown in Fig. 1(b)), then we say that the humanoid is not dynamically balanced. Further, let us assume the link L^1 consists of two links, link L^{1A} and link L^{1B} , connected via the joint J^0 (Fig. 1(c)). In the examples shown in Figs. 1(a) and 1(b), the joint J^0 is locked, so that links L^{1A} and L^{1B} behave as a single solid body. If we assume that the joint J^0 is also active, the terminal link will be dynamically balanced only if link L^{1A} remains immobile with respect to the ground, as presented in Fig. 1(c). In this case, link L^{1B} may move like any other link (L^2, L^3 or L^4), and need not be in contact with the ground.

In the double support phase of the gait, both feet are in contact with the support ground surface. In this case, a humanoid is dynamically balanced if at least one robot foot, or the foot's terminal link, is immobile and in full contact with the ground surface. Thus, for a humanoid to be dynamically balanced while in the double support phase, the CoP location of at least one foot has to be within its foot support region. This implies that the ZMP is inside the overall support area. If it happens that the CoP point reaches a foot's edge, then a moment that tends to overturn the foot or terminal link is generated.^{1,14-16} If one foot rotates, the walker is still dynamically balanced if the other foot or terminal link remains flat on the ground. However, even if both feet start to turn about their edges, resulting in a system that is dynamically unbalanced, the robot will not necessarily fall down. Namely, after some time of imbalance one or both feet may restore their full contact and thus dynamic balance may be restored.

As an example, consider a walker with a one-link foot. Sometimes, during the single support phase, such a walker may give up dynamic balance before the heel strike of the leading foot. Although the trailing foot rotates about its toe edge, the robot does not collapse and fall because of the eventual heel strike of the leading foot. Such a temporary period of imbalance is acceptable. An extreme example is a bipedal robot with point feet or curved feet. Such a robot is always in a state of dynamic imbalance, and the ZMP does not exist. For such cases, foot placement and the control of whole-body angular momentum are the only strategies that the robot can exploit to maintain successful walking in the presence of disturbances. In the next section, we discuss whole-body angular momentum control to improve disturbance rejection in humanoid walking.

2.2. CMP

The CMP,^{4,17–22} ground reference point is defined as follows. The CMP location, r_{CMP} , is defined as the point where a line parallel to the ground reaction force, passing through the whole-body CM, intersects with the ground surface. This condition can be expressed mathematically by requiring that the cross product of the CMP-CM position vector and the ground reaction force vector vanish, or

$$[(r_{\text{CMP}} - r_{\text{CM}}) \times F]_{\text{hor}} = 0. \quad (2)$$

By expanding this cross product, the CMP location can be written in terms of the CM location and the ground reaction force, or

$$x_{\text{CMP}} = x_{\text{CM}} - \frac{F_X}{F_Z} z_{\text{CM}} \quad \text{and} \quad y_{\text{CMP}} = y_{\text{CM}} - \frac{F_Y}{F_Z} z_{\text{CM}}. \quad (3)$$

Since the CMP point is a ground reference point, $z_{\text{CMP}} = 0$ at all times. Here the coordinate frame is oriented by the right hand rule with the z -axis directed vertically from the ground surface, the y -axis pointing in the direction of the walking motion (anterior–posterior direction), and the x -axis pointing to the right of the humanoid (medial–lateral direction). When the CMP departs from the ZMP, there exist nonzero horizontal CM moments, causing variations in whole-body angular momentum. While the ZMP cannot leave the ground support base,^e the CMP can — but only when horizontal moments act about the CM.

Horizontal ground reaction forces can be separated into zero-moment and moment components.¹⁹ The horizontal component (hor) of the total moment about the CM ($T_{\text{CM}}|_{\text{hor}}$) may be expressed as

$$T_{\text{CM}}|_{\text{hor}} = [(r_{\text{ZMP}} - r_{\text{CM}}) \times F]_{\text{hor}} = \left. \frac{dL}{dt} \right|_{\text{hor}}, \quad \text{or} \quad (4a)$$

^eWhen in single support, the *support base* is the outline of the part of the stance foot that is actually in contact with the ground. When in double support, where both feet are on the ground, the *support base* is the smallest convex shape that includes all points where both feet are in contact with the ground.

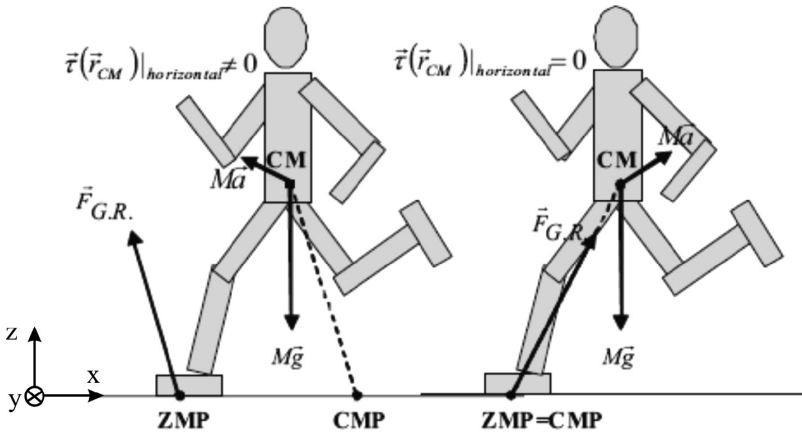


Fig. 2. The CMP and the relation between the ZMP and the CMP. $T_{CM}|_{hor} = \tau(r_{CM})|_{hor}$ is the horizontal component of the total moment about the CM.

$$T_x = [(y_{ZMP} - y_{CM}) \cdot F_z + z_{CM}F_y] = \frac{dL_x}{dt}, \tag{4b}$$

$$T_y = [(-z_{CM}) \cdot F_x - (x_{ZMP} - x_{CM})F_z] = \frac{dL_y}{dt}, \tag{4c}$$

where F is the ground reaction force and r_{ZMP} is the ZMP location on the ground surface. Equation (4) can be solved for the horizontal ground reaction forces, or

$$F_x = \underbrace{\left\{ \frac{F_z}{z_{CM}}(x_{CM} - x_{ZMP}) \right\}}_{F_x^{zero\text{-}moment}} + \underbrace{\left\{ -\frac{T_y}{z_{CM}} \right\}}_{F_x^{moment}}, \tag{5}$$

$$F_y = \underbrace{\left\{ \frac{F_z}{z_{CM}}(y_{CM} - y_{ZMP}) \right\}}_{F_y^{zero\text{-}moment}} + \underbrace{\left\{ \frac{T_x}{z_{CM}} \right\}}_{F_y^{moment}}, \tag{6}$$

where T_x and T_y are the CM moments in the mediolateral (x) and anterior–posterior (y)-directions, respectively. We call the control strategy that uses the zero-moment force component to exert a horizontal CM force, a zero-moment strategy, and the control strategy that uses the moment force component, a moment strategy.¹⁹ The moment forces of Eqs. (5) and (6) can be written in terms of the ZMP and CMP ground reference points, or

$$F_x^{moment} = -F_z \frac{x_{ZMP} - x_{CMP}}{z_{CM}}, \tag{7}$$

$$F_y^{moment} = F_z \frac{y_{ZMP} - y_{CMP}}{z_{CM}}. \tag{8}$$

As highlighted by Eqs. (7) and (8), the moment restoring force can be controlled by modulating the separation distance between the ZMP and the CMP.

Zero CM moment ($ZMP = CMP$) is not a general feature across all human movement tasks. For some movement patterns, humans purposefully generate angular momentum to enhance stability and maneuverability.^{21–23} By actively rotating body segments (arms, torso, legs), CM moments can be generated which cause horizontal moment forces to act on the CM, as defined by Eqs. (4) and (5). This strategy allows humans to perform movement tasks that would not otherwise be possible. For example, while balancing on one leg, humans are capable of repositioning the CM just above the stance foot from an initial body state where the CM velocity is zero, and the ground CM projection is outside the foot support envelope.^{f,22} Such a stability feature cannot be achieved using a bipedal control scheme that simply applies a zero-moment, inverted pendulum control. Clearly, if the ground CM projection falls outside the support envelope and the CM velocity is zero, the zero-moment force does not act to restore the CM position, but rather continually accelerates the CM away from the stance foot. This fact can be easily verified by reviewing the zero-moment force component from Eq. (5), or $F_x^{\text{zero-moment}} = F_z \cdot (x_{CM} - x_{ZMP})/z_{CM}$.

Imagine the case where a person is trying to balance on his right leg, and a laterally directed force disturbance causes x_{CM} to move beyond the foot envelope in a lateral, positive direction. Since x_{ZMP} cannot extend beyond the foot's lateral edge, $x_{CM} - x_{ZMP}$ is positive, making the CM zero-moment force positive, and causing the CM to move farther from the stance foot. The only way a person can successfully balance on one leg from these initial conditions is to actively generate angular momentum. By rotating the arms, trunk, head and swing leg, a CM moment in the positive y -direction can be generated, causing a negative moment force, $F_x^{\text{moment}} = -T_y/z_{CM}$, that can restore the CM to a position directly over the stance foot. This behavior can be observed in tightrope walking. Here body segments are accelerated to generate angular momentum about the CM and to create a moment force that restores the CM position over the stance foot.

Recently, a moment-exploiting control (MEC) approach for humanoid robots was developed that exploits both moment and zero-moment strategies to effectively modulate the horizontal force on the robot's CM so as to redirect the CM toward a desirable state.^{22–24}

3. Description of Mechanical Structures of the Mechanisms

In this section we describe the kinematic schemes of the robot's mechanical structure employed in the present work (Fig. 3). The basis for deriving the mechanism's mathematical model is the software for forming the dynamic model of a branched (open or closed) kinematic chain whose links are interconnected with joints having only one degree of freedom (DOF).

^fThe *support envelope* is the support base when the foot is flat on the ground during single support, or when both feet are flat on the ground during double support.

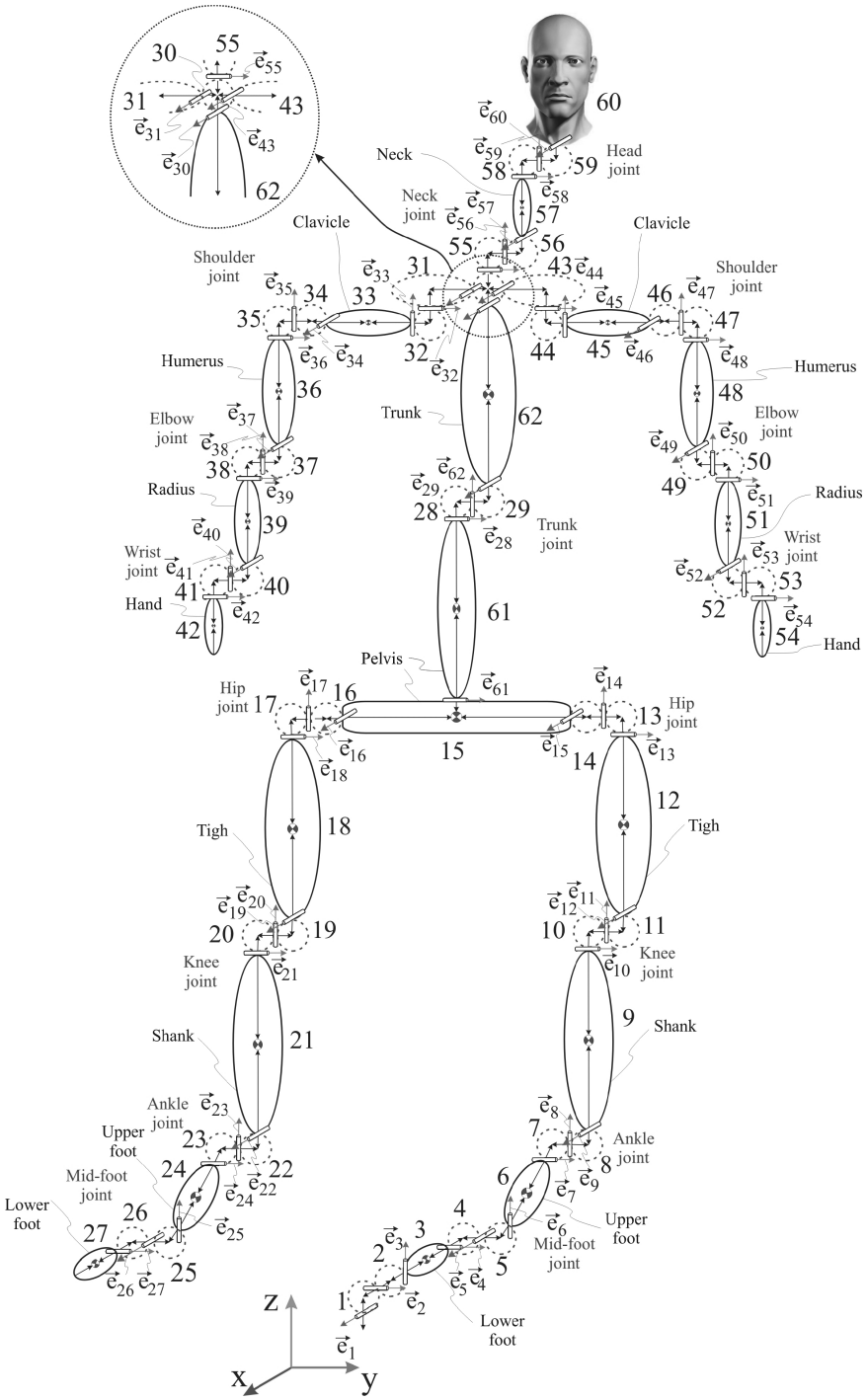


Fig. 3. Schematic of the robot's basic mechanical configuration having 62 DOFs.

Int. J. Human. Robot. 2008.05:639-678. Downloaded from www.worldscientific.com by MASSACHUSETTS INSTITUTE OF TECHNOLOGY on 07/10/13. For personal use only.

The mechanism is supported on the left leg. The first kinematic chain represents the legs (links 1–27), the second chain extends from the pelvis and comprises the trunk and the right arm (links 61, 28, 29, 62, 30–42), the third chain (links 43–54) forms the left shoulder and arm, and the fourth chain (links 55–60) forms the neck and head (Fig. 3).

The multi-DOF joints were modeled as a set of "fictitious" links (massless links of zero length) interconnected with the joints having one DOF. For example, the hip joints, which are in reality spherical joints with three DOFs, are modeled as sets of three one-DOF joints whose axes are mutually orthogonal. Thus, the left hip is modeled by the set of simple joints 13, 14 and 15 (with the unit rotation axis vectors e_{13} , e_{14} and e_{15}), and the right hip by the set of joints 16, 17 and 18 (the unit vectors e_{16} , e_{17} and e_{18}). The links connecting these joints (for the left hip links 13 and 14, and for the right hip links 16 and 17) were needed only to satisfy the mathematical formalism of modeling a kinematic chain. The other links (those that are not part of the joints with more DOFs) whose characteristics correspond to the links of an average human body (link 9 corresponds to the shank, link 12 to the thigh, etc.) are presented in Fig. 3 by solid lines. In the same figure, the above-mentioned "fictitious" links are represented by dashed lines.

Of special importance is the way of modeling the foot–ground contact in order to determine the exact position of the ZMP during the motion and observe the moment when the mechanism is out of dynamic balance. The loss of dynamic balance means that the mechanism collapses by rotating about one of the edges of the supporting foot, and this situation, obviously, has to be prevented. The contact of the mechanism with the ground is modeled by two rotational joints, determined with the unit vectors e_1 and e_2 (Fig. 3), which are mutually perpendicular. At the ZMP for a dynamically balanced motion, it is constantly ensured that $M_y = 0((M_x \perp M_y) \wedge (M_x, M_y \in XoY))$. It should be especially emphasized that the mechanism feet were modeled as the two-link ones. In Fig. 3, the anterior part of the left foot (toes) is presented by link 3, and its main part (foot body) by link 6. The toes of the right foot are presented by link 27 and the foot body by link 24.

The mechanism's dynamic parameters were determined so as to be as close as possible to those of the human experimental subject. The feet and hands were modeled as rectangular boxes. The shanks, thighs, forearms and upper arms were modeled as truncated cones. The pelvis–abdomen link and the thoracic link were modeled as elliptical slabs. The neck was modeled as a cylinder and the head was modeled as a sphere. Based on the links' dimensions, the links' masses and densities and CM positions were modeled to closely match the experimental values.

4. Experiment

Three healthy adults volunteered for the study. For this pilot investigation, each participant was asked to stand on his left foot, and lean to his left until his shoulder touched a support. The support was a flat force sensor, and the participant was

asked to lean until this sensor measured approximately 20 N of force. This level of force corresponded to a leaning posture where the CM projection on the ground surface fell outside the stance foot envelope. The support was then suddenly pulled away and motion recorded. For each study participant, a total of ten trials were collected.[§]

5. Data Acquisition

Kinetic and kinematic data were collected at the Holodeck Gait Laboratory of the Computer Science and Artificial Intelligence Lab at MIT, in a study approved by the MIT Committee on the Use of Humans as Experimental Subjects.

The data collection procedures were based on standard techniques. An infrared camera system (VICON 512) was used to measure the three-dimensional locations of reflective markers at 120 frames per second. A total of 33 markers were placed on various parts of a participant's body: 16 lower body markers, 5 trunk markers, 8 upper limb markers and 4 head markers. The VICON 512 system was able to detect marker positions with a precision of ~ 1 mm. Ground reaction forces were measured synchronously with the kinematic data at a sampling rate of 120 Hz using a force platform (Advanced Mechanical Technology Inc., Watertown, Massachusetts). The platform's ground reaction force and ZMP location were measured at a precision of ~ 0.1 N and ~ 2 mm, respectively.

The whole-body CM position was computed from the kinematic data. The ZMP and the ground reaction force intensity were obtained from the force plate.

6. Simulation

The initial posture (in which the humanoid is leaning by the left shoulder against the "wall"), and as the final ("normal") posture of free standing on one leg are taken from the experiment. The simulation starts from the moment when the humanoid loses support at the left shoulder. The system detects the endangerment of dynamic balance and attempts to preserve it. If the humanoid succeeds, it should return to the usual position of free standing on one leg without making contact with the environment except, naturally, via the supporting leg. The humanoid's behavior in the course of simulation is solely a consequence of the control employed.

The compensating action can be split into the following three phases:

- *Phase 1.* Here, the primary aim is to preserve dynamic balance, i.e. prevent the fall. This phase begins with the occurrence of the disturbance and ends when the CM projection comes "significantly" close to the ZMP position, i.e. when it becomes less than 0.003 m.

[§]From 30 recorded movements we selected a "sufficiently average" one to compare with it the simulation results. From this, we adopted the initial humanoid's posture from which simulation begins, and the terminal one to which the system converges in the last phase.

- *Phase 2.* This is the “calming down” phase. It lasts until the deviation of the instantaneous ZMP position becomes less than 0.001 m.
- *Phase 3.* In this phase the system returns to the “normal” position of standing on the one (left) leg.

Each of these phases has its control priorities and specificities. What is common to all the above phases is the constant concern of maintaining dynamic balance. This means that in each phase care is taken to control the actual position of the ZMP, on the basis of which the most appropriate control strategy is selected. The control strategy is different in the case where there is a danger that the ZMP is coming too close to the edge of the support area from that where the ZMP is “heading for” its reference position. In every phase, the control signal is formed in the same way: the value of the control signal in the subsequent iteration is obtained by adding to the control signal from the previous phase a corrective part formed depending on the phase. Hence, the formula for obtaining the control in the subsequent moment is of the form

$$u_j(i+1) = u_j(i) + \Delta u_j, \quad (9)$$

where the subscript j stands for the ordinal number of the humanoid joint DOF, i is the ordinal number of the iteration in the simulation (in fact, the subscript i represents time flow) and Δu_j is the correction added to the control quantity. The values adopted for the control quantities at each of the joints (j) in the initial moment $u_j(i=0)$ are those holding for the instant just before the obstacle removal. As mentioned above, the way of calculating Δu_j is different in each of the phases.

In the first two phases, there is no target (reference) posture of the humanoid to which it tends during the motion. The instantaneous posture depends on the initial position and the control applied. In the third phase, in which the humanoid returns to the “normal” one-leg standing position, there exists a target (reference) posture to which the humanoid is tending.

Each of these phases will be discussed in detail in the text to follow. It is understandable that compensation can be made in different ways. Our primary aim was to achieve the compensation performed in a manner similar to that of humans. This simulation case was named Case 1.

6.1. *Phase 1: Case 1*

The first phase starts with the appearance of the disturbance (removal of the “wall”). The moment when the system starts to react to the disturbance (when the active control action should begin) may be determined in two ways. One is to detect the decrease in the reaction force at the shoulder and the other is to detect the increase in the ZMP deviation from its “rest” position, i.e. the position before the disturbance occurred. This position we will also call the reference position.

In this study we use the increase in the ZMP deviation in the y -direction with respect to the reference position (which has been determined in advances and kept at the same position during the whole simulation). When the ZMP departs “sufficiently” from its reference position (i.e. when the ZMP deviation in the y -direction becomes larger than 0.001 m), the humanoid starts to react to the disturbance, i.e. starts to compensate for it. The compensation task is assigned to only some of the DOFs. We assume that Δu_j becomes different from zero at the following DOFs: 7, 9, 10, 13, 15, 16, 28, 62 and 46. At the other DOFs, a constant control signal is applied during the whole simulation period, the same as it was at each of the DOFs in the initial moment of simulation. Compensation is carried out in two mutually orthogonal planes — sagittal and frontal. The motion in the sagittal plane is enabled by those joints (DOFs) whose rotational axes are parallel to the x -axis (the system’s motion left–right), whereas the movements of the links in the frontal plane are enabled by the joints whose axes of rotation are parallel to the y -axis (the system’s motion forward–backward). Table 1 gives a summary of the DOFs with the joints they belong to, as well as the coordinate axis to which the rotation axes of the particular DOFs are parallel. The position of each DOF at the humanoid joints can also be seen from Fig. 3, showing the robot’s basic mechanical structure.

By the action of the joints listed in Table 1, the ZMP deviation in the corresponding direction is compensated for. Thus, if the rotation axis of the given DOF is parallel to the x -axis, the ZMP deviation is compensated for in the y -direction (in the expression to follow, this deviation is denoted as ΔZMP_y), i.e. if the rotation axis is parallel to the y -axis, the ZMP deviation in the x -direction (denoted as ΔZMP_x) is compensated for. The ZMP deviation is determined as the departure of the instantaneous ZMP position from its reference position (defined in advance), projected onto the corresponding axis.

The formula for calculating Δu_j at joints is of the following form:

- for the joints whose axes are parallel to the y -axis,

$$\Delta u_j = K_{P_j} \cdot \Delta ZMP_x(i) + K_{I_j} \cdot \sum_{k=1}^i \Delta ZMP_x(k) + K_{D_j} \frac{\Delta ZMP_x(i) - \Delta ZMP_x(i - 1)}{\Delta t}; \tag{10}$$

Table 1. Joints at which compensation is performed.

DOF	Joint	Rotation Axis	DOF	Joint	Rotation Axis
9	Ankle	x -axis	7	Ankle	y -axis
15	Hip	x -axis	10	Knee	y -axis
16	Hip	x -axis	13	Hip	y -axis
62	Trunk	x -axis	28	Trunk	y -axis
46	Shoulder	x -axis			

Table 2. Feedback gain coefficients per joint (Phase 1 — Case 1).

	Coefficient of the Positional Gain K_P	Coefficient of the Integral Gain K_I	Coefficient of the Derivative Gain K_D
Joint and ordinal number of the DOF — rotation about the x -axis			
Ankle — DOF 9	510	1.5	12
Hip — DOF 15	-2600	-2.6	-26
Hip — DOF 16	-2800	-2.6	-28
Trunk — DOF 62	-2800	-2.8	-28
Shoulder — DOF 46	3300	3.3	33
Joint and ordinal number of the DOF — rotation about the y -axis			
Ankle — DOF 7	-37	-0.035	-0.35
Knee — DOF 10	-33	-0.033	-0.33
Hip — DOF 13	-37	-0.035	-0.35
Trunk — DOF 28	-800	-0.8	-8

- for the joints whose axes are parallel to the x -axis,

$$\Delta u_j = K_{P_j} \cdot \Delta ZMP_y(i) + K_{I_j} \cdot \sum_{k=1}^i \Delta ZMP_y(k) + K_{D_j} \frac{\Delta ZMP_y(i) - \Delta ZMP_y(i-1)}{\Delta t}, \tag{11}$$

where j denotes the ordinal number of the DOF and i the ordinal number of the simulation iteration. In Table 2 are given the values of the coefficients K_P, K_I and K_D for each particular DOF used in (10) and (11).

It is evident from Table 2 that not all feedback gain coefficients that compensate for the ZMP deviation at the DOFs whose rotation axes are parallel to the x -axis (joints 9, 15, 16, 62 and 46) are of the same sign. This means that on the basis of the same ZMP deviation the compensating rotations of the joints 9 and 46 will be in one direction, and those of the joints 15, 16 and 62 in the opposite direction, which will be commented later. The feedback gains for the compensation of the ZMP deviation for the joints whose rotation axes are parallel to the y -axis are of the same sign.

It was also necessary to provide the capability of bringing down the humanoid’s body by bending the supporting leg knee. This was performed in a way similar to what humans do. As can be seen from the stick diagram in Fig. 4, the knee is bent (the humanoid does not stand upright on the supporting leg). Bearing in mind that the leg bending at the knee should not cause additional bending of the part of the humanoid above it, it is necessary to simultaneously ensure the appropriate motion of both the ankle and the trunk. Because of that, the Δu_j for the joints 7, 10 and 13 is formed by adding to Eq. (9) the term $\Delta u_j^{\text{knee bend}}$, so that the formula for

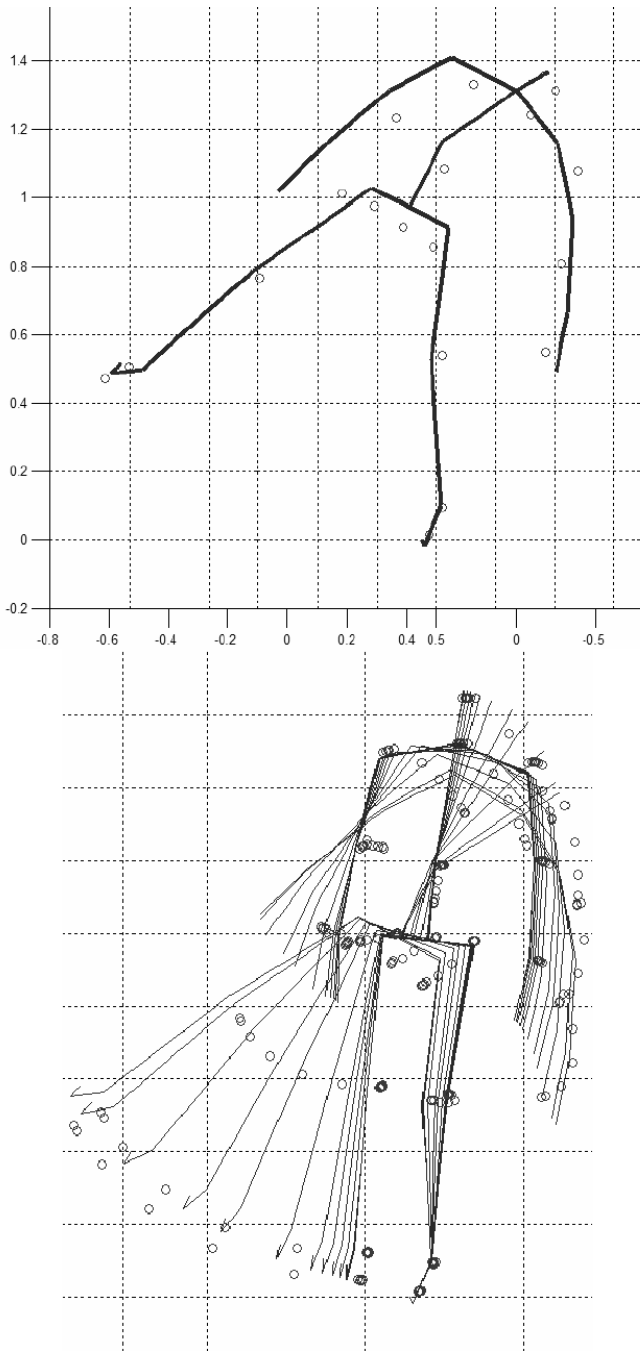


Fig. 4. Case 1: Stick diagram of the humanoid posture at the end of the first phase and the beginning of the second phase. The circles show the positions of the markers on the subject's body in the experiment. The bottom picture shows the sequence of postures in the process of reaching the final posture at the end of the first phase.

calculating the controls at the joints is of the form

$$u_j(i + 1) = u_j(i) + \Delta u_j + \Delta u_j^{\text{knee bend}}, \tag{12}$$

where the term $\Delta u_j^{\text{knee bend}}$ depends on the deviations of the internal coordinates at the trunk and the hip with respect to the reference posture of the system attained at the end of the simulation. In other words, the larger the inclination of the trunk and hip joint with respect to the “normal” posture, as well as the rate of the leg’s lateral swing, the greater the knee bending to be performed by the mechanism.

The internal coordinates participating in this control are q_{15}, q_{16}, q_{62} , and \dot{q}_{15} . Their deviations are calculated with respect to $q_{\text{ref}15}, q_{\text{ref}16}, q_{\text{ref}62}$, and $\dot{q}_{\text{ref}15}$. These values were taken from the “normal” standing posture, to which the humanoid converges during the third phase. Hence, we take into account the deviations at the trunk joint (DOF 62), the supporting leg hip (DOF 15), the hip of the swing leg (DOF 16) and the deviation rate of the supporting leg hip (DOF 15). The formula for calculating $\Delta u_j^{\text{knee bend}}$ is

$$\begin{aligned} \Delta u_j^{\text{knee bend}} &= K_{P_{q_{15}}} \cdot \Delta q_{15}(i) + K_{I_{q_{15}}} \cdot \sum_{k=1}^i \Delta q_{15}(k) + K_{D_{q_{15}}} \frac{\Delta q_{15}(i) - \Delta q_{15}(i - 1)}{\Delta t} \\ &\quad + K_{P_{q_{16}}} \cdot \Delta q_{16}(i) + K_{I_{q_{16}}} \cdot \sum_{k=1}^i \Delta q_{16}(k) + K_{D_{q_{16}}} \frac{\Delta q_{16}(i) - \Delta q_{16}(i - 1)}{\Delta t} \\ &\quad + K_{P_{q_{62}}} \cdot \Delta q_{62}(i) + K_{I_{q_{62}}} \cdot \sum_{k=1}^i \Delta q_{62}(k) + K_{D_{q_{62}}} \frac{\Delta q_{62}(i) - \Delta q_{62}(i - 1)}{\Delta t} \\ &\quad + K_{P_{\dot{q}_{15}}} \cdot \Delta \dot{q}_{15}(i). \end{aligned} \tag{13}$$

Table 3 lists the values of the coefficients used in Eq. (13).

As can be seen from the table, the coefficients at the joint 10 (knee) are of the opposite sign to those at the joints 7 and 13 (ankle and hip) since the changes of the angles at the hip and ankle in the squat are of the opposite sign to the change of the angle at the knee.

With the feedback gains selected this way and control laws defined by Eqs. (9)–(13), the compensating motion of the humanoid in the first phase is very similar to that of the tested subject, as is evident from Fig. 4. In this figure (considering the same time instant), the circles represent the positions of the markers on the subject’s body in the experiment, whereas the stick diagram obtained by simulation is shown by the solid line. It is evident that the degree of similarity between the simulated

Table 3. Coefficients used in the knee bending realization (Phase 1 — Case 1).

DOF	$K_{P_{q_{15}}}$	$K_{I_{q_{15}}}$	$K_{D_{q_{15}}}$	$K_{P_{q_{16}}}$	$K_{I_{q_{16}}}$	$K_{D_{q_{16}}}$	$K_{P_{q_{62}}}$	$K_{I_{q_{62}}}$	$K_{D_{q_{62}}}$	$K_{P_{\dot{q}_{15}}}$
7	1.62	0.0027	0.108	1.62	0.0027	0.108	2.43	0	0.756	0.1
10	-3.24	-0.0054	-0.216	-3.24	-0.0054	-0.216	-4.86	0	-1.56	-0.2
13	2.295	0.0297	1.08	2.295	0.0297	1.08	1.485	0.0027	0.405	0.1

and experimentally recorded motions is very high. The ZMP position obtained by simulation and experiment, projection of the CM of the overall system, and the CMP position during the simulation are shown in Fig. 7. As this figure is related to the whole movement, and not only to its first phase, it will be discussed somewhat later.

A very important contribution to the ground reaction force is the mass of the overall system. Hence it is natural to expect that the ZMP position is close to the system's CM projection on the ground surface. In this case, this was not fulfilled at the beginning of the experiment, so that it was expected that the compensating action would bring about their convergence, while the control system had to constantly "take care" of maintaining dynamic balance.

The first phase terminates when the CM comes "sufficiently" close to the actual ZMP position, i.e. when the distance between the two points becomes smaller than 0.003 m. At this point, the second phase begins.

6.2. Phase 2: Case 1

Since the direct threat of overturning has been eliminated, and there are no other urgent tasks, in the second phase the humanoid prepares for the third phase of returning to the initial posture. Hence the actual ZMP approaches its reference position in order to most effectively realize the third phase. The second phase lasts until the deviation of the actual ZMP position becomes "sufficiently" small, i.e. until the deviation of the instantaneous ZMP position from the reference becomes smaller than 0.001 m.

Figure 5 shows the stick diagram of the humanoid position at the end of the second phase. The control is synthesized in the same way as in the first phase (formulas (9)–(11)), but with the changed values of the feedback gains per joint. The values of K_P , K_I and K_D for the second phase are listed in Table 4.

6.3. Phase 3: Case 1

By the end of the second phase, the humanoid has completely resolved the problem of dynamic balance and, since it is unnatural for it to remain in the position occurring at the end of the second phase (Fig. 6(a)), it enters the third phase, in which the system, without disturbance, is to pass from one posture to another and remain in it. In Fig. 6(a), the posture to be attained is shown by the thin line, and in Fig. 6(b), the posture attained at the end of simulation is shown. It is clear that during the whole of the third phase, apart from passing from one posture to the other, it is necessary to constantly take care of dynamic balance.

Hence, in the third phase, the formula (10) becomes

$$u_j(i+1) = u_j(i) + \Delta u_j + \Delta u_j^{\text{loc}}. \quad (14)$$

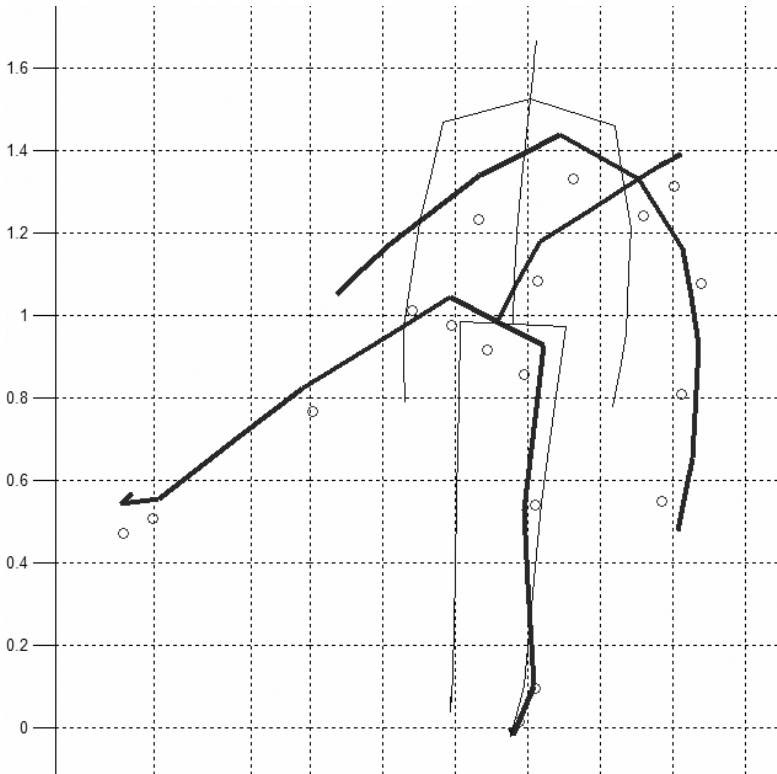


Fig. 5. Case 1: Stick diagram of the humanoid posture at the end of the second phase and the beginning of the third phase. The circles show the positions of the markers on the subject's body in the experiment.

Table 4. Feedback gains per joint (Phase 2 — Case 1).

	Coefficient of the Positional Gain K_P	Coefficient of the Integral Gain K_I	Coefficient of the Derivative Gain K_D
Joint and ordinal number of the DOF — rotation about the x -axis			
Ankle — DOF 9	50	0.05	5
Hip — DOF 15	-200	-0.1	-10
Hip — DOF 16	-200	-0.1	-10
Trunk — DOF 62	-100	-0.1	-6
Shoulder — DOF 46	40	0.3	3
Joint and ordinal number of the DOF — rotation about the y -axis			
Ankle — DOF 7	-20	-0.012	-1.25
Knee — DOF 10	-10	-0.005	-0.5
Hip — DOF 13	-17	-0.015	-1.5
Trunk — DOF 28	-400	-0.4	-4

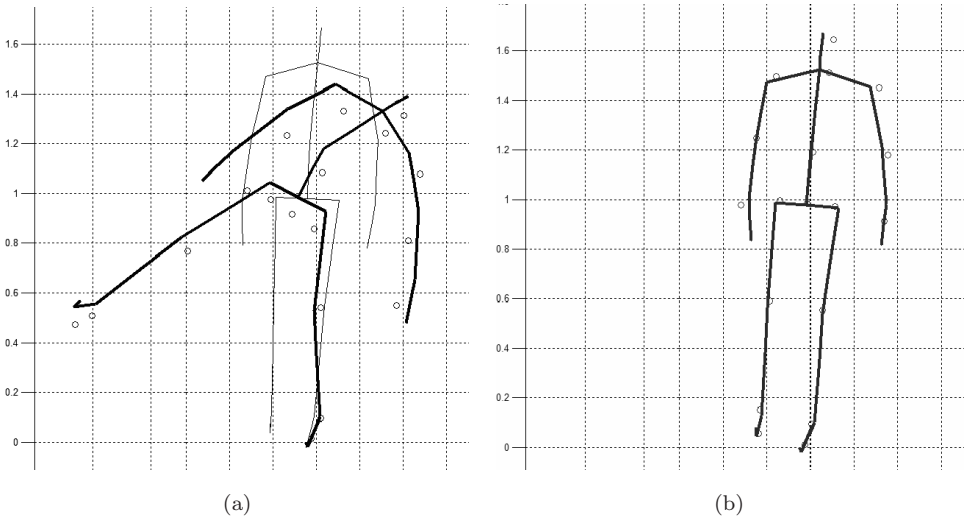


Fig. 6. (a) Case 1: Stick diagram of the mechanism posture at the beginning of the third phase (solid line). The thin line shows the mechanism target posture at the end of the third phase, to which the mechanism is to converge. (b) Mechanism posture at the end of the third phase.

During the third phase, apart from the regulator for maintaining dynamic balance, use is also made of the local regulators at all DOFs that participated in the compensating actions in the previous phases.

The component Δu_j is formed in the same way as before (based on the expressions (2) and (3)), and the coefficients are the same as in Table 4. The control component Δu_{loc} is applied only at the joints that have been active in the previous phases, i.e. 7, 9, 10, 13, 15, 16, 28, 62 and 46, and it is formed in the following way:

$$\Delta u_{loc_j} = K_{P_{loc_j}} \cdot \Delta q_j(i) + K_{I_{loc_j}} \cdot \sum_{k=1}^i \Delta q_j(k) + K_{D_{loc_j}} \frac{\Delta q_{j_x}(i) - \Delta q_{j_x}(i-1)}{\Delta t}, \quad (15)$$

where the subscript j denotes the ordinal number of the corresponding DOF, whereas $\Delta q_j(i)$ stands for the deviation of the internal angle of the corresponding joint from the reference value in the i th iteration of simulation. The feedback gains are the same for all the joints, and they are $K_{P_{loc_j}} = 0.1$, $K_{I_{loc_j}} = 0.001$ and $K_{D_{loc_j}} = 0.01$.

Figure 7 shows the trajectories of the ZMP, CMP and CM during all three phases. In the initial instant, the CMP and the CM coincided and were located outside the support area. It can rightly be said that the applied control has effectively been “driving” them to the center of the support area.

Let us consider in more detail the mutual relationships between the ZMP, CMP and CM projection on the ground during the whole experiment. In Fig. 8 are shown

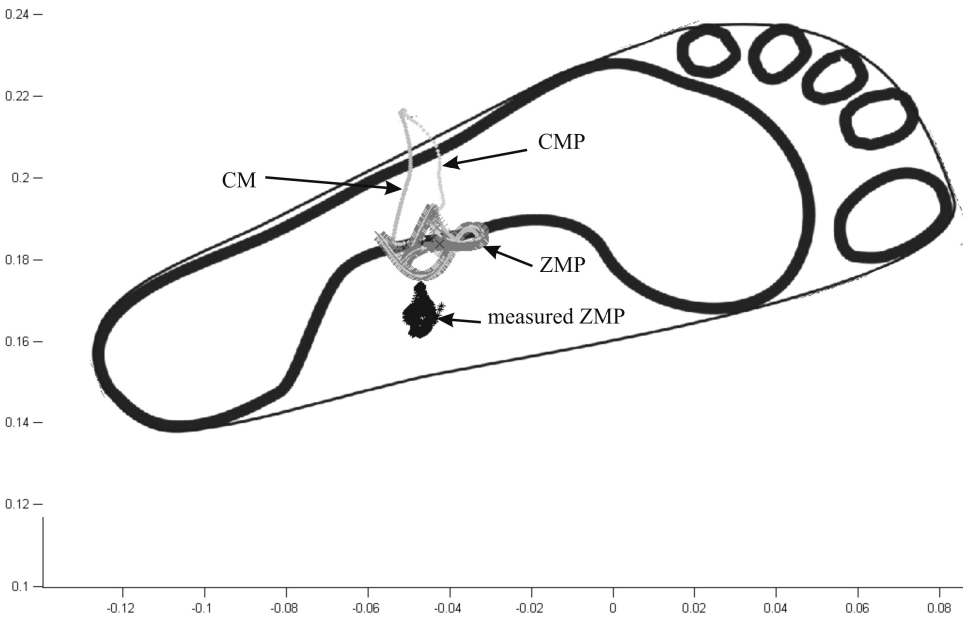


Fig. 7. Case 1: Positions of the ZMP, CMP and ground projection of the system's CM and measured CoP (ZMP)^h in all three phases.

the calculated positions of the ZMP, CMP and ground CM projection, as well as the ZMP position acquired in the experiment with the human subject in four different time instants: at the beginning and in the middle of the first phase, and at the beginning of the second and the third phase. At the beginning (Fig. 8(a)), the CMP and CM projection coincide. This may occur only if the reaction force is vertical or very close to the vertical. This is obviously so if we bear in mind that the humanoid was initially immobile, standing on one leg, and that the foot area was very small. Besides, in the initial moment the CM projection is outside the support area, which unambiguously speaks of the necessity to apply a compensating action as soon as the humanoid has lost support.

The compensating action applied drove the CMP and CM closer to the center of the support area, and their positions in the middle of the first phase are shown in Fig. 8(b). It is evident that the CMP moved faster. This only means that there appeared a more significant horizontal component of the reaction force, which is understandable since the humanoid, while performing the compensating action, also moves. In the course of the second and third phases, the mutual convergence of the ZMP, CMP and CM continued, approaching the reference ZMP position.

In the previous example the aim was to synthesize a control that would ensure the realized compensating movement in a way to be as close as possible to that of

^hIn the case of dynamically balanced humanoid posture, the ZMP and the CoP coincide.

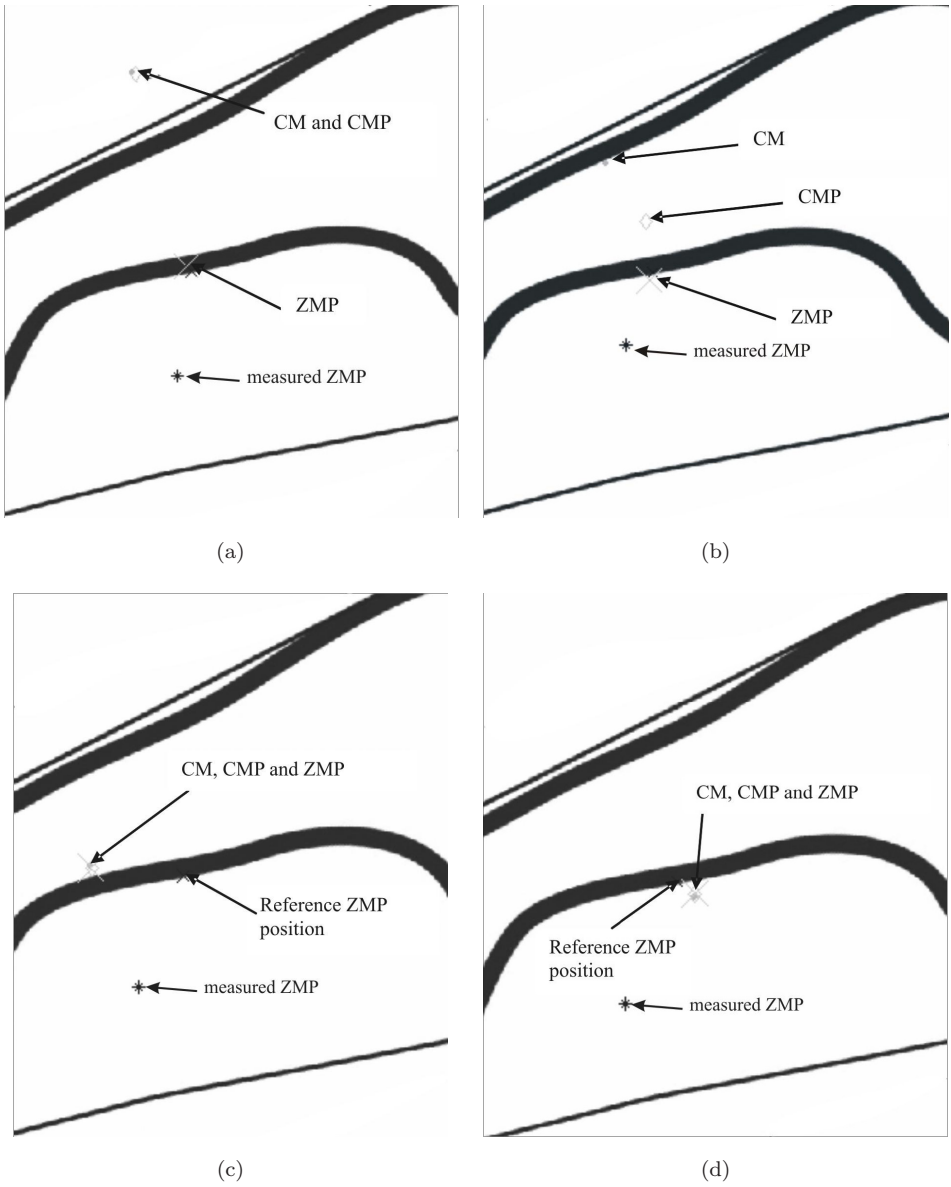


Fig. 8. Case 1: Mutual relationships between the ZMP, CMP and CM projection on the ground: (a) beginning of the first phase, (b) middle of the first phase, (c) beginning of the second phase, and (d) beginning of the third phase.

the subject recorded in the experiment. However, the expectation that the joints having parallel axes all behave the same way in the compensation of deviations was not fulfilled. Namely, some of these joints acted in one direction and some in the opposite direction. We will illustrate this with the example of the joints 9, 15, 16, 46

and 62, whose rotation axes are parallel to the x -axis, and all these joints are active in the compensation for the ZMP deviation in the lateral direction. If we look at Table 2, we can see that the coefficients K_P , K_I and K_D for the DOFs 9 and 46 have the sign “plus”, and the DOFs 15, 16 and 62 have “minus”. On the basis of this, one could derive a hasty conclusion that the joints 9 and 46 contribute to the convergence of the ZMP to its reference position, whereas the actions at the joints 15, 16 and 62 have an opposite effect. In other words, the hip and trunk joints (15, 16 and 62) “spoil” what the ankle and shoulder joints (DOFs 9 and 46) have achieved.

In order to shed more light on this problem we carried out several additional simulations but with the values for K_P , K_I and K_D changed. First, we simulated the compensating movement using the identical control laws as in the previous case, but with the signs of all the feedback gains for the joints 15, 16 and 62 made “plus”, so that they were: for the left hip (DOF 15) $K_P = +2600$, $K_I = +2,6$ and $K_D = +26$; for the right hip (DOF 16) $K_P = +2800$, $K_I = +2,6$ and $K_D = +28$; and for the trunk (DOF 62) $K_P = +2800$, $K_I = +2,8$ and $K_D = +28$. Thus, all the joints acted simultaneously in the same way. We call this Case 2. The results are presented in Figs. 9– 11. Figure 9 shows the trajectories of the ZMP, CMP and CM-a obtained by simulation, and of the ZMP positions measured during the experiment; Fig. 10 shows the mechanism’s postures at the beginning of the first, second and third phases and at the end of the simulation; whereas Fig. 11 shows relative positions

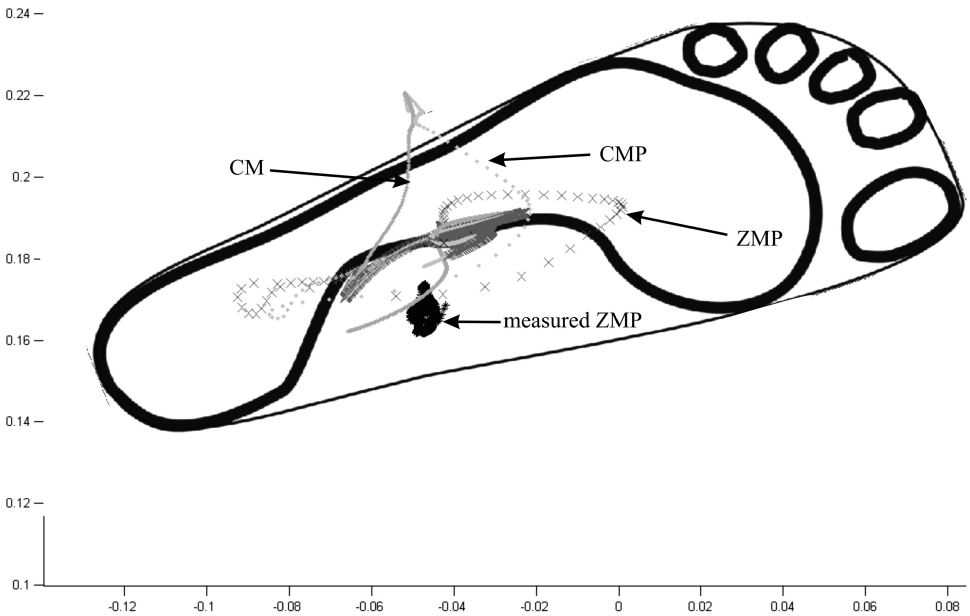


Fig. 9. Case 2: Positions of the ZMP, CMP and ground projection of the system’s CM and measured CoP (ZMP) in all three phases.

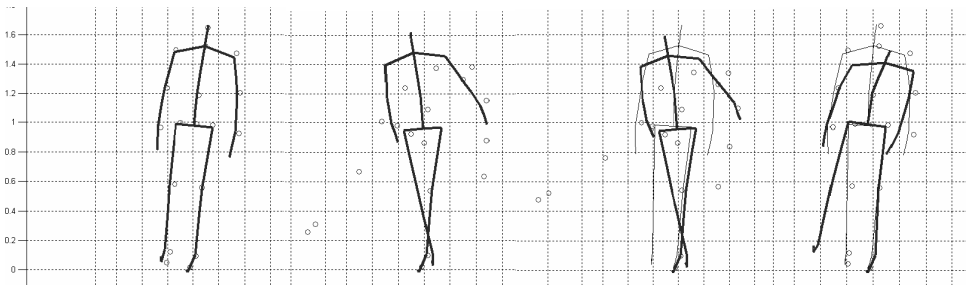


Fig. 10. Case 2: Stick diagram of the humanoid's postures at the beginning of the first, second and third phases. As before, the circles show the positions of the markers on the subject's body in the experiment.

of the ZMP, CMP and CM projection on the ground during simulation and the measured position of the ZMP during the experiment.

It is evident from Figs. 9 and 10 that the trajectories of the ZMP and CMP, as well as of the projection of the system's CM on the ground, are more scattered than in Case 1, which indicates a lowered capability of the fine control of the ZMP and CMP positions and CM projection on the ground. But the system still preserved dynamic balance. It can also be seen that there was no swinging aside of the right leg, but rather crossing of the legs occurred. Such a posture is extremely undesirable because of the possibility of tripping and falling. In Ref. 2, such postures were called potentially dangerous configurations, and they are, obviously, inadmissible.

The third case we considered (Case 3) is identical to Case 2 (all the coefficients have the sign "plus"), but the values of the coefficients K_P , K_I and K_D for the first and second phases (Tables 5 and 6) are better-adjusted. The coefficients for the local regulator in the third phase were not changed (they remained identical in all the three cases).

Simulation results are shown in Figs. 12–14.

It is clear that the process of compensation has been improved compared to the previous case. Namely, it is visible that the trajectories of the ZMP, CMP and CM projection "calmed down" (Figs. 12 and 14), and that no "potentially dangerous configuration" appeared during the first, second or third phase (Fig. 13). The final posture attained at the end of the simulation is very close to the target one.

Recall that Case 1 represents the simulation by which we succeeded in obtaining a high degree of similarity of the humanoid's behavior to that of the subject under the action of disturbances, whereas in the simulations presented in Cases 2 and 3, we attempted to shed some additional light on the fact that some joints may "counteract each other".

Finally, we attempt to highlight the problem of the choice of action of particular joints. In the task of "bringing the ZMP closer" to the reference position were assigned the task of "moving it away" and vice versa (in Case 1, the coefficients K_P , K_I and K_D for the DOFs 9 and 46 had the sign "plus", and for the DOFs

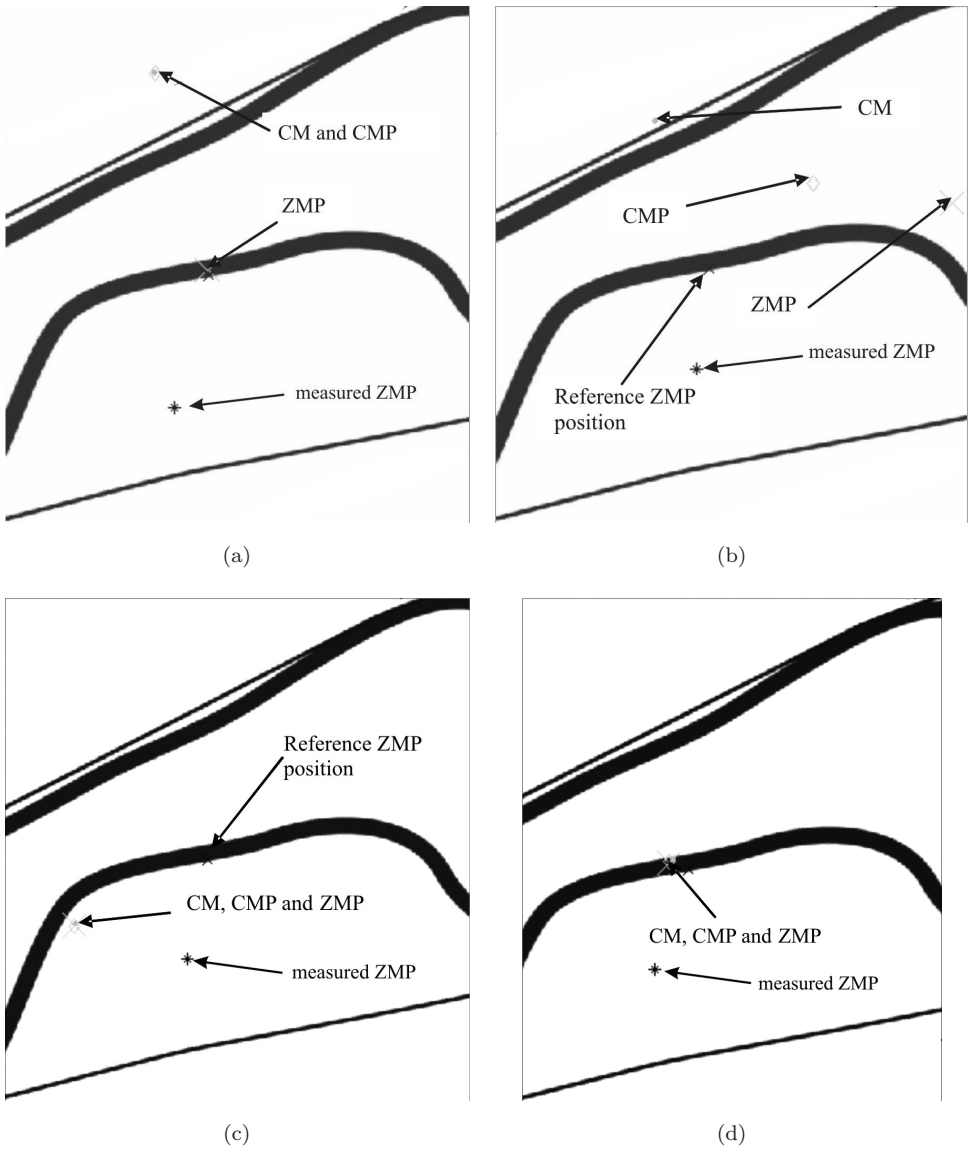


Fig. 11. Case 2: Mutual relationships between the ZMP, CMP and CM projection on the ground: (a) beginning of the first phase, (b) middle of the first phase, (c) beginning of the second phase, and (d) beginning of the third phase.

15, 16 and 62 “minus”). In order to get an answer to this question, we inverted the signs of all the active joints (joints participating in the compensation) of the legs whose rotation axes are parallel to the x -axis (DOFs 9 15, 16, 46 and 62). Now the coefficients K_P, K_I and K_D for the DOFs 9 and 46 have the sign “minus”, and the DOFs 15, 16 and 62 “plus”. The DOFs 9 and 46 still act in the same direction and

Table 5. Feedback gains per joint (Phase 1 — Case 3).

	Coefficient of the Positional Gain K_P	Coefficient of the Integral Gain K_I	Coefficient of the Derivative Gain K_D
Joint and ordinal number of the DOF — rotation about the x -axis			
Ankle — DOF 9	280	2.8	28
Hip — DOF 15	120	0.12	1.2
Hip — DOF 16	120	0.12	1.2
Trunk — DOF 62	130	0.13	1.3
Shoulder — DOF 46	1	0.01	0.1
Joint and ordinal number of the DOF — rotation about the y -axis			
Ankle — DOF 7	-17	-0.035	-3.5
Knee — DOF 10	-17	-0.033	-3.3
Hip — DOF 13	-17	-0.035	-3.5
Trunk — DOF 28	-17	-0.35	-3.5

Table 6. Feedback gains per joints (Phase 2 — Case 3).

	Coefficient of the Positional Gain K_P	Coefficient of the Integral Gain K_I	Coefficient of the Derivative Gain K_D
Joint and ordinal number of the DOF — rotation about the x -axis			
Ankle — DOF 9	12	0.01	0.1
Hip — DOF 15	8	0.001	0.1
Hip — DOF 16	8	0.001	0.1
Trunk — DOF 62	11	0.0011	0.11
Shoulder — DOF 46	0.05	0.0005	0.005
Joint and ordinal number of the DOF — rotation about the y -axis			
Ankle — DOF 7	-10	-0.04	-0.4
Knee — DOF 10	-10	-0.04	-0.4
Hip — DOF 13	-10	-0.04	-0.4
Trunk — DOF 28	-10	-0.04	-0.4

the DOFs 15, 16 and 62 in the opposite direction. However, all the DOFs act in the opposite direction with respect to those in Case 1. This case was termed Case 4.

The basic observation is that the system has lost dynamic balance. For Case 4, Fig. 15 shows the trajectories of the ZMP, CMP and CM-a obtained by simulation and of the ZMP positions measured during the experiment. Figure 16 shows the stick diagrams of the humanoid's postures at the beginning of the first, second and third phases and at the moment when the system lost dynamic balance during the third phase. It is evident that already in the course of the first phase, a potentially

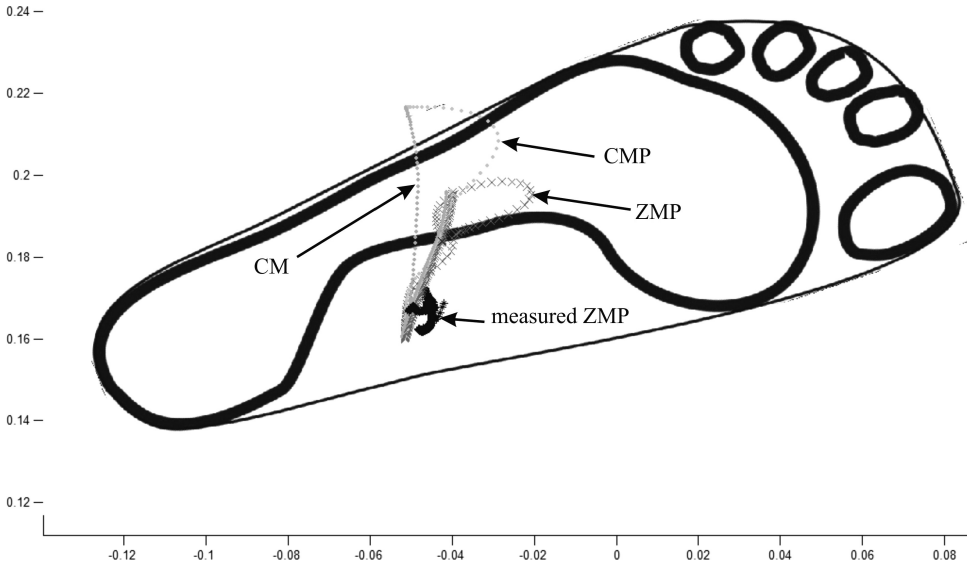


Fig. 12. Case 3: Positions of the ZMP, CMP and ground projection of the system's CM and measured CoP (ZMP) in all three phases.

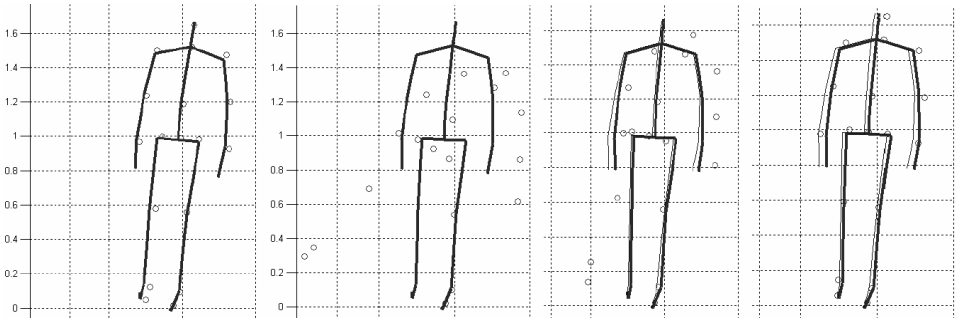


Fig. 13. Case 3: Stick diagram of the humanoid's postures at the beginning of the first, second, and third phases, respectively. As before, the circles show the positions of the markers on the subject's body in the experiment.

dangerous configuration appeared, which was, however, difficult to realize, bearing in mind the admissible motion at the joints. Also, dynamic balance was not preserved. Hence it is quite clear that this case is unsuitable for compensation, and as such it does not deserve further attention.

Let us focus our attention on Cases 1–3. It should be noted that the biped locomotion system should always take care to remain in an upright position and that its constant task is to preserve dynamic balance, which was strictly observed during the simulation. The overall control strategy of preserving and maintaining dynamic balance is based on the ZMP. It was assumed that the ZMP position can

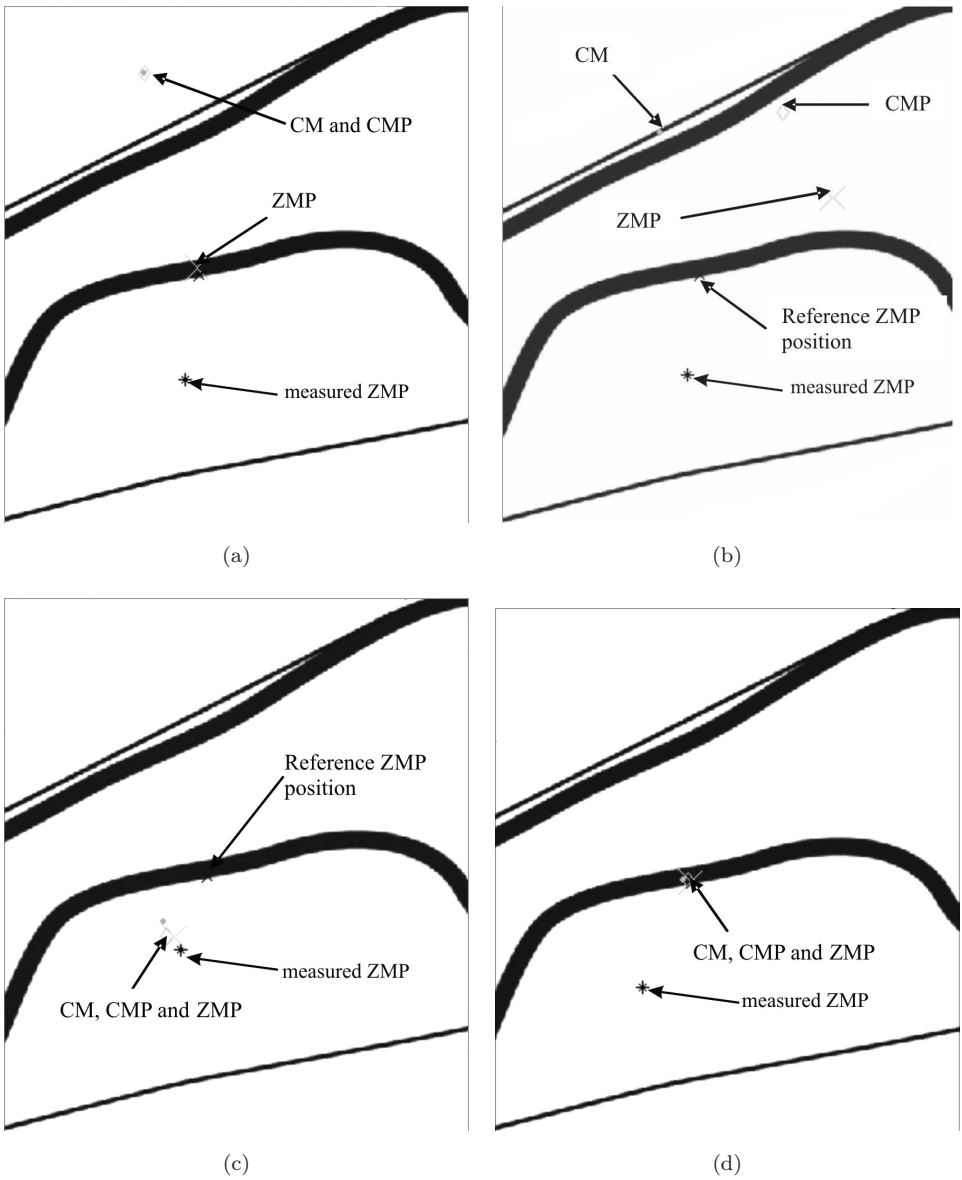


Fig. 14. Case 3: Mutual relationships between the ZMP, CMP and CM projection on the ground: (a) beginning and (b) middle of the first phase, (c) beginning of the second phase, and (d) beginning of the third phase.

be measured in real time (which is a valid assumption) and this information and desired ZMP position serve as the basis for definition and realization of the compensating action. This enabled effective counteraction of the large (Phase 1) and small (Phase 2) disturbances. In each of the three cases considered (Cases 1–3), dynamic

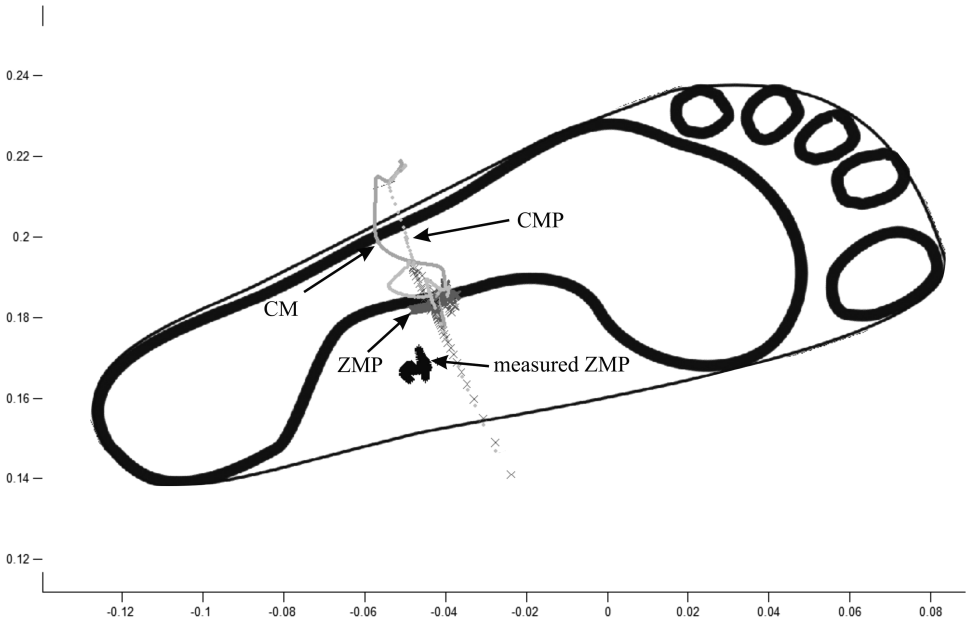


Fig. 15. Case 4: Positions of the ZMP, CMP and ground projection of the system's CM and measured CoP (ZMP) in all three phases.

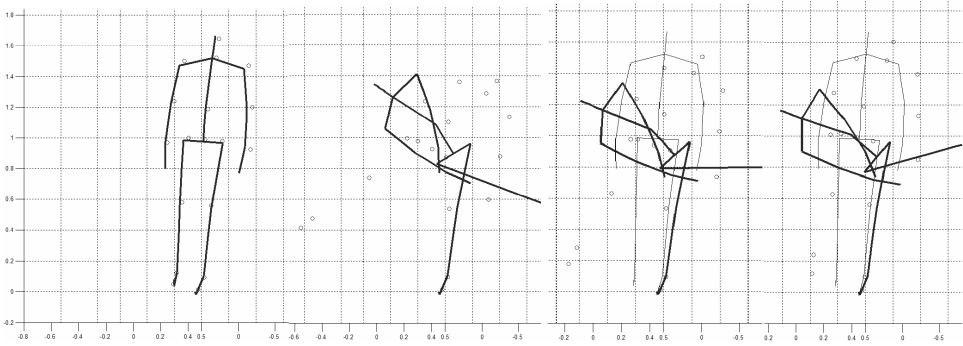


Fig. 16. Case 4: Stick diagrams of the humanoid's posture for the beginning of the first, second and third phases and for the moment when the system lost its dynamic balance during the third phase, respectively. As before, the circles show the positions of the markers on the subject's body in the experiment.

balance was preserved. Besides, we can see that the ZMP is kept close to the center of the support area and that the CMP (because of the minimization of the moment tending to rotate the system) very rapidly converges to the ZMP; the CM projection too tends to the ZMP, since the contribution of the CM to the intensity and position of the action point of the ground reaction force is very significant.

Bearing in mind that in all three cases (Cases 1–3) dynamic balance has been preserved, a question arises as to the evaluation of the quality of the control actions in each of these cases. The question can be phrased in another way: Why did nature choose just the compensating movement described in Case 1?

To give a reliable answer to this question we will consider the driving torques at the joints in each of the mentioned cases.

In Figs. 17–21 are shown the corresponding joint driving torques. The black solid line shows the torques at the joints for Case 1 (humanoid behavior shown in Figs. 4–8); the gray dotted line shows the torques for Case 2 (Figs. 9–11); the black dotted line shows the torques at the joints for Case 3 (Figs. 12–14); and the gray solid line shows the torques at the joints for Case 4 (Figs. 15 and 16).

It can be seen that the torques' intensities for almost all joints (Cases 1–3 are compared) are the smallest for Case 1, which, according to the movement realized,

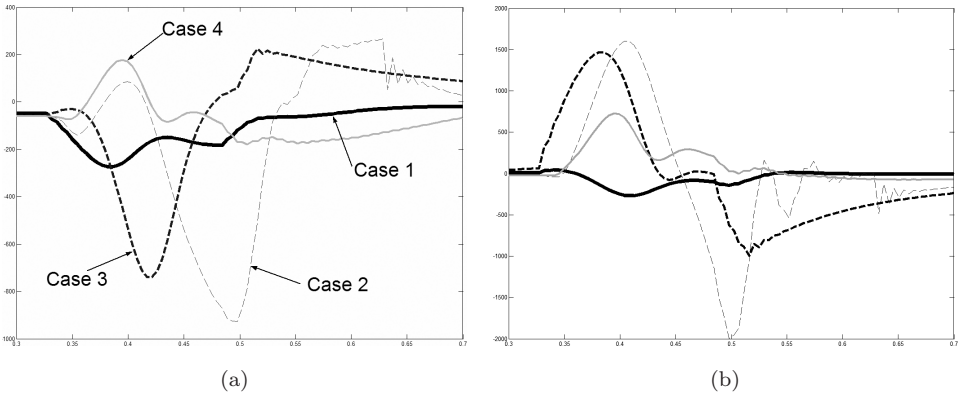


Fig. 17. Torques at the ankle for Cases 1–4: (a) DOF 7, (b) DOF 9.

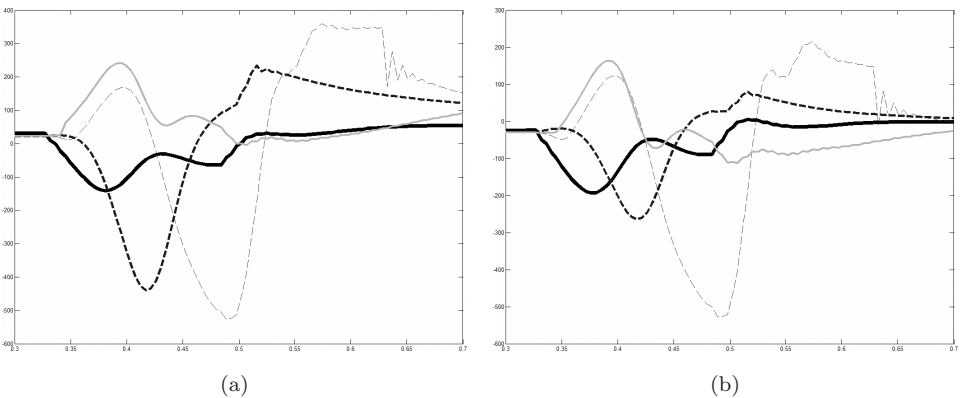


Fig. 18. Torques at the knee and left hip for Cases 1–4: (a) DOF 10 — knee; (b) DOF 13 — left hip.

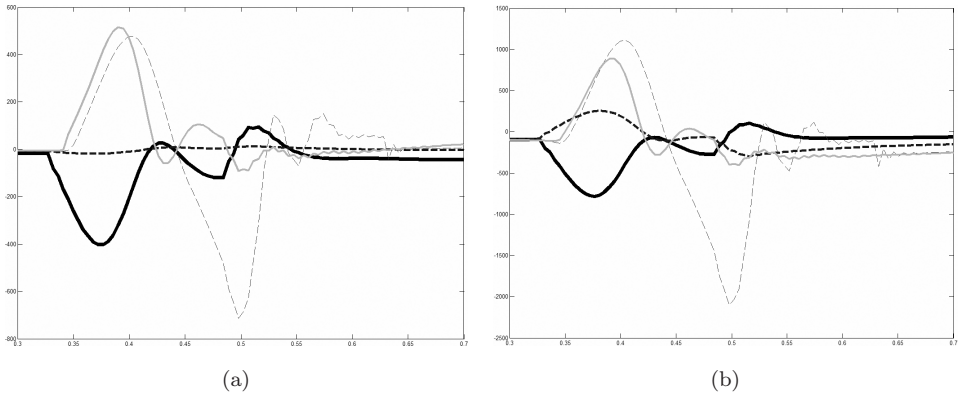


Fig. 19. Torques at the left and right hips for Cases 1–4: (a) DOF 15 — left hip; (b) DOF 16 — right hip.

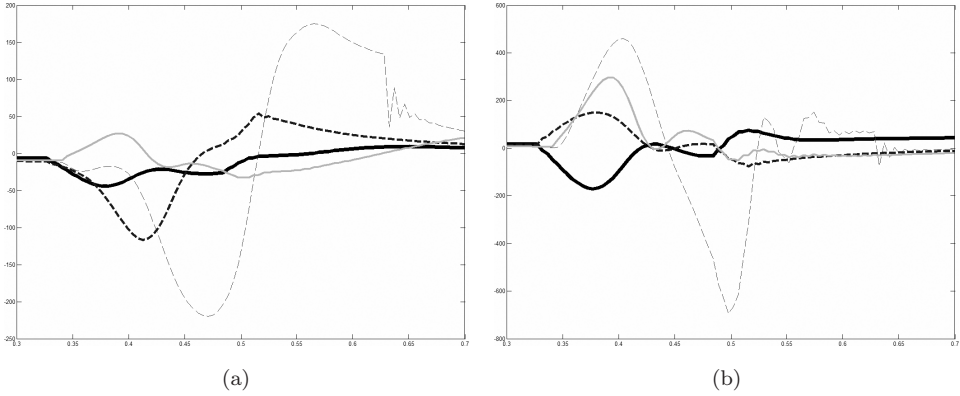


Fig. 20. Torques at the trunk for Cases 1–4: (a) DOF 28 — trunk in the frontal plane; (b) DOF 62 — trunk in the sagittal plane.

is closest to that by which a human compensates for this type and intensity of disturbances. Only at the right hip (Fig. 19(b)) is the moment intensity significantly smaller in Case 3 compared to Cases 1 and 2. The reason for this is that Cases 1 and 3 do not represent the same movement. In Case 3, there is no swinging out of the right leg.

However, in deciding which compensating action is to be applied, several criteria have to be simultaneously taken into account.

One of the important criteria is certainly the plausibility of the motion with respect to: (a) the geometric characteristics, i.e. the allowable range of the motion at each particular joint involved; and (b) the capabilities of the particular joint actuators to realize the given movement. Here, it is necessary to take into account the fact that the movement cannot be realized if the motion in at least one joint has not been performed as planned. Besides, when choosing one of the more possible

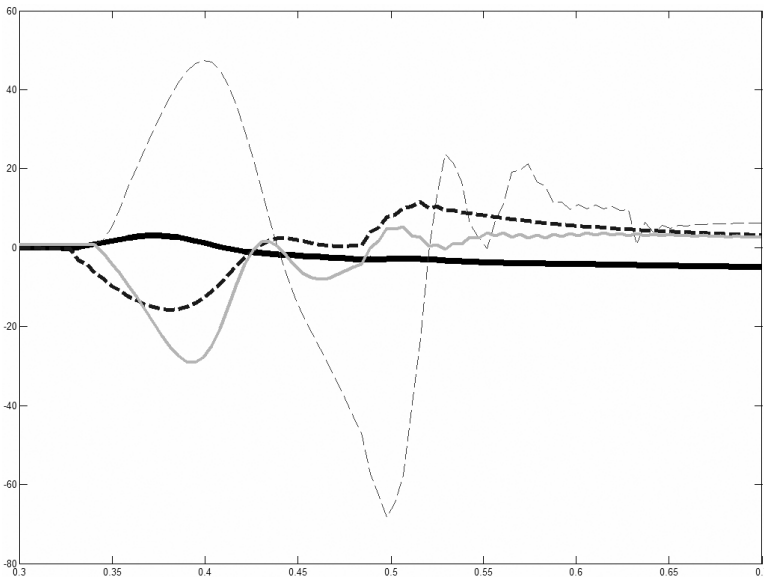


Fig. 21. Torques at the left shoulder (DOF 46) for Cases 1–4.

compensating movements that are realizable, the movement with smaller driving torques at the joints (especially if the driving torques are not close to the muscles' limits, i.e. the actuators' limits) will certainly have priority. In other words, the movements that are more comfortable in the sense of the efforts are obviously more desirable.

The other criterion is related to the occurrence of “potentially dangerous configurations”. Such states of the mechanism are utterly undesirable, because the unusual motion of the limbs may cause the unplanned humanoid's collision with the environment or with itself, leading to the biped overturning despite the correct functioning of its control system. In order to avoid the potentially dangerous configurations as much as possible, a human learns to realize the compensating movements in a certain way, such as by moving the limbs away from the body, to prevent self-collision.

Let us consider now some of the possible benefits that accrue from the realization of the compensating movements at the ankle and hip joints in the sagittal plane in opposite directions (Case 1).

Recall that the ZMP position is influenced by all the forces acting on the humanoid: gravity forces and forces arising due to motion (for example, inertial forces). The driving torques at the joints arising from the gravity forces depend only on the instantaneous positions of the joints (i.e. joint angles), whereas the weights of the particular links are constant. Therefore, it is clear that the intensities of the moments due to gravity forces change only because of the change of the position of the joints (the intensities and directions of the gravity forces are constant) and

only the change of the joint positions can influence the ZMP position. On the other hand, the intensities of the forces arising from the motion depend on the characteristics of the motion of the links, so that the moments of these forces depend on the instantaneous intensities and directions of the forces and instantaneous positions of the joints. In order for the forces arising from the motion to influence the ZMP position in a desired way, it is necessary to simultaneously take care of the influences of all the changeable quantities, i.e. the directions and intensities of the forces and the distance from the point for which the moment is calculated. Hence, it is quite clear that it is much more difficult to control the ZMP position by forces arising from the motion than by gravity forces. Obviously, to make control of the ZMP more efficient, it would be useful to diminish the influence of the forces arising from motion, and thus augment the influence of the gravity forces. This is possible to achieve via the rotation of two successive joints in opposite directions. This way, the influence of the forces arising from the motion can be significantly reduced.

Therefore, the first benefit of the compensating movements performed by the ankle and hip in the sagittal plane in opposite directions accrues from the inertial effects, which, thanks to the opposite directions of rotation, are partly self-canceled, and their overall effect is lowered. Hence the contribution of the moments due to gravity forces becomes more significant.

Besides, due to the motion of the ankle and hip in opposite directions, the moments arising from gravity forces are also partly canceled, so that the resulting change of the moments that influence the ZMP position is the difference between the change of the moments due to the change of the ankle and hip positions. In other words, to the same change of joint angles corresponds a smaller change of the resulting moments that influence the change of the ZMP position, allowing thus its finer adjustment.

The other effect that we want to address is the influence of the Coriolis forces on the loads at the joints. If the directions of angular velocities at the hip and ankle joints are opposite (Fig. 22), the direction of Coriolis acceleration is opposite to the gravity forces, lowering thus the joint loads, which can be considered as a favorable effect. In the case of the same direction of angular velocities, the load increases.

Taking into account all of the above discussion, it is clear why Case 1 is more acceptable than Cases 2 and 3.

However, it should be mentioned that the compensation in Case 3 represents how humans react for such disturbances, but when these disturbances are of smaller intensity and not too large, driving torques at the joints are required. Then, such disturbances belong to the class of small disturbances, and examples concerning these cases can be found in Ref. 2.

7. Conclusion

In this investigation we considered the situation of a study participant leaning against a support while standing on one leg. When the support was suddenly

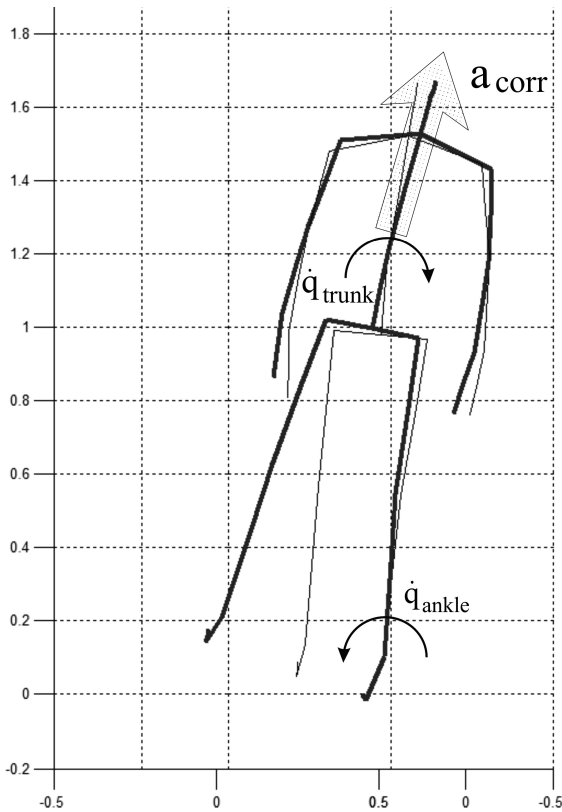


Fig. 22. Direction of the Coriolis force for the opposite directions of angular velocities at the ankle and hip.

removed, the participant succeeded in moving his whole-body CM from a position outside the support envelope to within the support base by rotating his head, trunk, arms and swing leg to generate angular momentum. Kinetic and kinematic data were recorded throughout the movement task. In order to gain insight into the control laws applied, a humanoid model was developed with realistic mass distribution and degrees of freedom. By applying three different phases to the control synthesis, the human model was controlled to closely mimic the observed human movement pattern.

The experimental tests and modeling allowed us to make the following observations and conclusions. All three ground reference points studied in this investigation (the CMP, ZMP and CM projection on the ground) are critical determinants of CM horizontal force. For the zero moment force component (inverted pendulum, $ZMP = CMP$), the ZMP and CM projection are important ground reference points, whereas for the moment force component, the ZMP and CMP ground points are key indicators. In our test, given that the ZMP is inside the support base, and the CM starts outside the support envelope with zero velocity, it is not possible that the

CM can be brought back over the support base without the purposeful generation of angular momentum about the CM. This is indicated by the fact that the CMP is initially divergent from the ZMP, moving outside the base of support. However, once the CM ground projection point was brought back within the support base, horizontal CM forces were applied primarily by an inverted pendulum, zero-moment strategy (ZMP = CMP). Throughout the entire movement task, the stance foot remained dynamically balanced and therefore did not rotate with the ZMP always positioned well inside the base of support.

Acknowledgments

This work was funded by the Ministry of Science of the Republic of Serbia under contract TR-6315B, and by the MIT Media Lab Consortia.

References

1. M. Vukobratović, B. Borovac and V. Potkonjak, Towards a unified understanding of basic notions and terms in humanoid robotics, *Robotica* **25** (2007) 87–101.
2. M. Vukobratović, B. Borovac, M. Raković, V. Potkonjak and M. Milinović, On some aspects of humanoid robots gait synthesis and control at small disturbances, *Int. J. Human. Robot.* **5**(1) (2008) 119–156.
3. H. Elftman, The function of the arms in walking, *Hum. Biol.* **11** (1939) 529–535.
4. M. Popovic, A. Hofmann and H. Herr, Angular momentum regulation during human walking: Biomechanics and control, in *Proc. IEEE Int. Conf. Robotics and Automation (ICRA)*, New Orleans, Los Angeles, USA (27–29 April, 2004) (IEEE Press), pp. 2405–2411.
5. J. B. Saunders, V. T. Inman and H. D. Eberhart, The major determinants in normal and pathological gait, *J. Bone Joint Surg. Am.* **35** (1953) 543–558.
6. S. A. Gard and D. S. Childress, The influence of stance-phase knee flexion on the vertical displacement of the trunk during normal walking, *Arch. Phys. Med. Rehab.* **80** (1999) 26–32.
7. G. Pratt, Low impedance walking robots, *Integ. Comput. Biol.* **42** (2002) 174–181.
8. B. Full and D. Koditschek, Templates and anchors: Neural mechanical hypotheses of legged locomotion on land, *J. Exp. Biol.* **202** (1999) 3325–3332.
9. M. Vukobratović, B. Borovac and K. Babković, Contribution to the study of anthropomorphism of humanoid robots, *Int. J. Human. Robot.* **2**(3) (2005) 361–387.
10. M. Vukobratović and D. Juričić, Contribution to the synthesis of biped gait, *Proc. IFAC Symp. Technical and Biological Problem on Control*, Erevan, USSR (1968).
11. M. Vukobratović and D. Juričić, Contribution to the synthesis of biped gait, *IEEE Trans. Bio-Med. Eng.* **16**(1) (1969).
12. D. Juričić and M. Vukobratović, Mathematical modeling of biped walking systems, *ASME Publ. 72-WA/BHF-13* (1972).
13. M. Vukobratović, *Legged Locomotion Systems and Anthropomorphic Mechanisms*, Mihajlo Pupin Institute, Belgrade (1975). Also published in Japanese (Nikkan Shim-bun, Tokyo), in Russian (MIR, Moscow, 1976) and in Chinese (Beijing, 1983).
14. M. Vukobratović and B. Borovac, Zero-moment point — Thirty five years of its life, *Int. J. Human. Robot.* **1**(1) (2004) 157–173.
15. M. Vukobratović and B. Borovac, Note on the article zero-moment point — Thirty-five years of its life, *Int. J. Human. Robot.* **2**(2) (2005) 225–227.

16. M. Vukobratović, B. Borovac and V. Potkonjak, ZMP: A review of some basic misunderstandings, *Int. J. Human. Robot.* **3**(2) (2006) 153–176.
17. H. Herr, A. Hofmann and M. Popovic, New horizons for orthotic and prosthetic technology: Merging body and machine, *ZIF Int. Conf. Walking Machines*, Bielefeld, Germany (2003).
18. A. Goswami and V. Kallem, Rate of change of angular momentum and balance maintenance of biped robots, *Int. Conf. Robotics & Automation*, New Orleans, Los Angeles, USA (2004), pp. 3785–3790.
19. M. Popovic, A. Hofmann and H. Herr, Zero spin angular momentum control: Definition and applicability, *IEEE-RAS/RSJ Int. Conf. Human. Robot.*, Santa Monica, CA, USA (November 2004).
20. M. Popovic, A. Goswami and H. Herr, Ground reference points in legged locomotion: Definitions, biological trajectories and control implications, *Int. J. Robot. Res.* **24**(10) (2005) 1013–1032.
21. H. Herr and M. Popovic, Angular momentum in human walking, *J. Exp. Biol.* **211** (2008) 467–481.
22. A. Hofmann, M. Popovic and H. Herr, Exploiting angular momentum to enhance bipedal center-of-mass control, *IEEE Trans. Robot. Autom.* (2008) (in press).
23. A. Hofmann, M. B. Popovic, S. Massaquoi and H. Herr, A sliding controller for bipedal balancing using integrated movement of contact and non-contact limbs, in *Proc. IEEE/RSJ Int. Conf. Intelligent Robots and Systems*, Sendai, Japan (2004), pp. 1952–1959.
24. H. M. Herr, A. G. Hofmann and M. B. Popovic, Biomimetic motion and balance controllers for use in prosthetics, orthotics and robotics. US Patent 7,313,463; United States Patent, Massachusetts Institute of Technology, Cambridge MA, Serial No. 499853, Series Code 11 (Filed 4 August, 2006; accepted 25 December, 2007).



Miomir Vukobratović was born in Botos, Serbia, in 1931. He received his B.Sc. and Ph.D. degrees in Mechanical Engineering from the University of Belgrade in 1957 and 1964, respectively, and a D.Sc. degree from the Mashinovedeniya Institute, Soviet (now Russian) Academy of Science, Moscow, in 1972. From 1968 to 1996, he was head of the Biodynamics Department, then director of the Laboratory for Robotics and Flexible Automation and director of the Robotics Laboratory, respectively, at the Mihailo

Pupin Institute.

He is a visiting professor teaching graduate courses in robotics at several universities in the former Yugoslavia and abroad. He is author/coauthor of more than 245 scientific papers in the field of robotics and system theory, published in leading international journals, as well as author/coauthor of about 360 papers in proceedings of international conferences and congresses. He has also authored/coauthored 15 research monographs published in English, Japanese, Russian, Chinese and Serbian, 2 advanced textbooks in robotics in English, and 10 chapters in international monographs. Among other accolades, he is a holder of the Joseph Engelberger Award in robotics (for his pioneering, internationally recognized results in applied research and education in robotics), conferred by the Robotic Industries Association, USA, in 1996.

Prof. Vukobratović is a full member of the Serbian Academy of Sciences and Arts, a foreign member of the Soviet (now Russian) Academy of Sciences, a full member of the International Academy of Nonlinear Sciences and several other foreign academies, president of the Yugoslav Academy of Engineering, a foreign member of the International Engineering Academy, Moscow, and foreign member of the Chinese Academy of Engineering and other national academies. He is *doctor honoris causa* of Moscow State University, named after M. V. Lomonosov, and several other universities in Europe. Based on the Citation Index, he has been cited about 2000 times.

His research interests include computer generation of dynamic models of manipulation and biped locomotion systems, dynamic robot control, modeling and control of robots in contact with the dynamic environment, performance control of active systems, constructions and structures.



Hugh M. Herr received a B.A. degree in Physics from Millersville University of Pennsylvania, USA, in 1990; an M.Sc. degree in Mechanical Engineering from MIT, USA, and Ph.D. degree in Biophysics from Harvard University, USA, in 1998. He is an Associate Professor within MIT's Program of Media Arts and Sciences, and the Harvard-MIT Division of Health Sciences and Technology. His primary research objective is to apply principles of biomechanics and neural control to guide the design of prostheses, orthoses and exoskeletons. He is the author of over 60 technical publications in biomechanics and wearable robotics, and is the recipient of the 2007 Heinz Award for Technology, the Economy and Employment.



Branislav Borovac was born in Leskovac, Serbia, in 1951. He received his M.Sc. and Ph.D. degrees in Mechanical Engineering from the University of Novi Sad, Serbia, in 1982 and 1986, respectively. He became Assistant Professor of Engineering Design in 1987, Assistant Professor of Robotics in 1988, Associate Professor of Robotics in 1993, and since 1998, he has been Professor of Robotics, all at the Faculty of Technical Sciences, University of Novi Sad. He is coauthor of two research monographs, published by Springer-Verlag (1990) and CRC Press (2001). He is author/coauthor of 30 scientific papers in the field of robotics, published in international journals, as well as author/coauthor of about 80 papers in proceedings of international conferences and congresses.

His research interests include biped locomotion, humanoids, robot modeling and control, industrial robotics, sensors and sensor information integration, force sensors and their use in contact tasks, assembly, mechatronics, product design and flexible systems.



Mirko Raković was born in 1982 in Sremska Mitrovica, Serbia. He graduated from the Faculty of Technical Sciences, University of Novi Sad, in 2005. Since then he has been working as a junior assistant at the Chair of Mechatronics, Robotics and Automation of the Faculty of Technical Sciences. His research interests are robotics, bipedal gait, mechatronics, and computer electronics and programming.



Marko Popovic received a B.Sc. degree in Physics from Belgrade University, Serbia (1995), an M.Sc. degree in Physics from Ohio State University, USA (1996), and a Ph.D. degree in Physics from Boston University, USA (2002). In 2001–2002, he was a postdoctoral fellow at Harvard University, and in the same year joined the MIT Biomechatronics Group as a postdoctoral associate. He has authored about 20 peer-reviewed publications, cited by about 250 other publications according to Google Scholar, in diverse fields such as physics, robotics, biomechanics and human-computer systems. Since Fall 2007, he has been working as a research scientist at MIT, and a lecturer at Belgrade University. His research interests include human biomechanics and humanoid robotic control.



Andreas Hofmann received an undergraduate degree from MIT, an M.Sc. degree from RPI, both in Electrical Engineering, and a Ph.D. degree from MIT in Computer Science. While a Ph.D. student in the MIT computer science department, working in the Biomechatronics Group at the MIT Media Lab, his research focused on the advancement of control systems that produce biomimetic walking motions while ensuring stability in the presence of significant disturbances. He is currently working at Vecna Technologies Inc., Cambridge, MA, USA.



Miloš Jovanović was born in 1967 in Majdanpek, Serbia. He received a B.Sc. degree at the Faculty of Electrical Engineering, Belgrade University, and an M.Sc. degree at the same faculty. He is working at the Robotic Center, Mihajlo Pupin Institute, in Belgrade, Serbia, as a senior researcher. His research interests are robotics, bipedal gait, mechatronics, and computer electronics and programming.



Veljko Potkonjak was born in Belgrade in 1951. He studied at the Faculty of Electrical Engineering, University of Belgrade, and graduated in 1974. The same year he was accepted for post-graduate studies at the same faculty, and he finished in 1977. In 1981, he defended his doctoral thesis. After graduation, Potkonjak started his work at the Faculty of Electrical Engineering, as an assistant in the field of mechanics. He became an assistant professor in 1985, and in 1990, he was promoted to the rank of associate professor, and finally in 1995 to the rank of full professor. During his educational career, he has been teaching Mechanics, Robotics and Biomechanics. He was also a teacher or a visiting researcher at the Faculty of Electronics, University of Nish, Serbia; the Technical Faculty in Cacak, Serbia; the National Technical University of Athens, Greece; and the American University of Athens.

The research interests of Prof. Potkonjak primarily concern robotics. In this field he received his M.Sc. and Ph.D. degrees. His attention has been oriented to problems concerning the dynamic modeling of robotic systems and the implementation of these models in design and control. He is author/coauthor of three international research monographs (in English; some of them translated into Japanese and Chinese), two chapters in *Handbook of Mechanical Systems Design*, several textbooks for universities and for secondary schools, 60 international journal papers, 26 papers in international conference, proceedings, and a number of papers in Yugoslav journals and conference proceedings. Prof. Potkonjak has made a large number of reviews for respected international journals and conferences as well as for domestic conferences. In the field of robotics and automation he was engaged in a large number of projects (research and commercial), sometimes as head and sometimes as participant.